MONOTONIC AND FATIGUE BEHAVIOR OF
2-D WOVEN CERAMIC MATRIX COMPOSITE
AT ROOM AND ELEVATED TEMPERATURES
(BLACKGLAS/NEXTEL 312)

THESIS

MUSA AL-HUSSEIN
LT.COL., ROYAL JORDANIAN AIR FORCE
AFIT/GAE/ENY/98S-01

DEPARTMENT OF THE AIR FORCE
AIR UNIVERSITY
AIR FORCE INSTITUTE OF TECHNOLOGY

Wright-Patterson Air Force Base, Ohio

AFIT/GAE/ENY/98S-01

MONOTONIC AND FATIGUE BEHAVIOR OF
2-D WOVEN CERAMIC MATRIX COMPOSITE
AT ROOM AND ELEVATED TEMPERATURES
(BLACKGLAS/NEXTEL 312)

THESIS

MUSA AL-HUSSEIN
LT.COL., ROYAL JORDANIAN AIR FORCE
AFIT/GAE/ENY/98S-01

AFIT/GAE/ENY/98S-01

MONOTONIC AND FATIGUE BEHAVIOR OF 2-D WOVEN CERAMIC

MATRIX COMPOSITE AT ROOM AND ELEVATED TEMPERATURES

(BLACKGLAS/NEXTEL 312)

THESIS

Presented to the Faculty of the School of Engineering

of The Air Force Institute of Technology

Air University

In Partial fulfillment of the

Requirements for the Degree of

Master of Science in Aeronautical Engineering

Musa H. Al-Hussein

LT.COL., Royal Jordanian Air Force
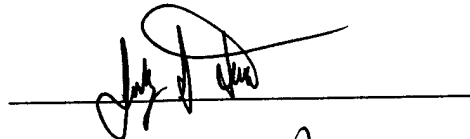
September 1998

MONOTONIC AND FATIGUE BEHAVIOR OF

2-D WOVEN CERAMIC MATRIX COMPOSITE

AT ROOM AND ELEVATED TEMPERATURES

(BLACKGLAS/NEXTEL 312)

MUSA AL-HUSSEIN, B.S., M.S.
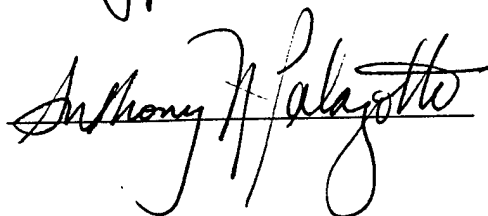LT COL, Royal Jordanian Air Force

Approved:

_____
Chairman

8/20/98
date

_____

8/20/98
date

_____

8/21/98
date

The views expressed in this thesis are those of the author and do not reflect the

official policy or position of the United States Air Force, the Department of Defense,

or the U.S. Government.

Preface

The purpose of this study was to investigate the behavior of a woven fabric reinforced ceramic matrix composite (CMC) at room temperature and at elevated temperature. The CMC was Blackglas/Nextel nitrided 312. Monotonic tensile and compressive tests, tension-tension, and tension-compression fatigue tests were carried out at room and elevated temperature. The elevated temperature was 760°C. The fatigue tests were carried out at load levels of 0.25 to 0.8 of ultimate tensile stress to develop the maximum stress versus the number of cycles to failure relationship of the material. The failure mechanisms in both monotonic and fatigue tests were investigated.

Table of Contents

List of Figures

List of Tables

Abstract

The purpose of this study was to investigate the performance of a woven fabric reinforced ceramic matrix composite under monotonic and fatigue loading conditions at room temperature and at elevated temperature. Specifically, the test had three objectives: (1) to determine the material characteristics under monotonic tensile and compressive loading at room temperature and at elevated temperature (760°C), (2) to determine the relationship between maximum stress levels and number of cycles to failure under tension-tension and tension-compression low frequency (0.1Hz) loading conditions at room and at elevated temperature, (3) to investigate the initiation and progression of damage mechanisms and failure modes under monotonic and fatigue loading conditions.

The composite used was a Blackglas/Nextel nitrided 312 woven fabric. Blackglas is a refractory silicon carboxide that is obtained by the pyrolysis of polysiloxane precursors. Nextel is an alumina-silica ceramic fiber composition containing up to 14 w/o boria. Monotonic tensile and compressive, fatigue tension-tension, and fatigue tension-compression tests were carried out at room temperature and at elevated temperature. Damage mechanisms, both initiation and progression, were evaluated based on this microscopic examination.

During room temperature monotonic tensile loading, the material exhibited an ultimate stress (σ_{ult}) of 69.24MPa and a proportional limit of 44MPa.; while at elevated temperature, it had an ultimate stress of 65.2MPa and a proportional limit of 24MPa. The

room temperature monotonic compressive test exhibited an ultimate stress of 273.9MPa, while in the elevated temperature monotonic compressive test the ultimate stress was found to be 334.4MPa. The proportional limit was the same as the ultimate stress in both compressive tests.

The damage in the room temperature tensile test initiated at the pores between the fill and warp. This was followed by transverse matrix cracking of the warp, leading to matrix cracking and severe fiber pull-out. In the elevated temperature monotonic tensile test, the failure initiated at the pores also, but with more fiber pull-out and interface debonding. This could be attributed to the effect of the high temperature on the matrix which became ductile. The fracture surface was more jagged in the elevated temperature monotonic tensile test.

The fracture surfaces in the monotonic compressive tests were very rough in both, room temperature and elevated temperature cases. The room temperature test had more fiber break and matrix damage in the fill and warp than the elevated temperature test. Damage was initiated at the pores in both the room temperature and elevated temperature tests. This was followed by matrix crushing which was noticed in the form of powder that came out of the fractured surfaces. Less damage was noticed in the matrix in the elevated temperature test; since the matrix became ductile.

Tension-tension (T-T) & tension-compression (T-C) fatigue tests were performed at different stress levels at room and elevated temperatures to develop maximum stress versus number of cycles to failure (S-N) relationship for the material. The S-N curves were compared to evaluate the effects of temperature, loading type, and stress level on the fatigue behavior of the material. S-N curves for the material showed that : (1) at room

temperature the number of cycles to failure in T-T were higher than in T-C for a given maximum stress level . The fatigue strength for 40,000 cycles for the room temperature T-T fatigue tests was about 48MPa, while it was 36MPa for the T-C fatigue tests, (2) at the elevated temperature there was no significant difference in the number of cycles to failure at a given maximum stress level between the T-T & T-C fatigue tests. The corresponding fatigue strength for both cases, under the elevated temperature, was about 24MPa.

The room temperature low cycle T-T test specimen fracture surface had two distinguished regions. One region was smooth, which was about 35% of the fractured surface cross section, while the second region was rough with a lot of fiber pull-out and formed 65% of the cross section. On the other hand, the room temperature high cycle T-T test specimen fracture surface section was smooth all over with no noticeable fiber pull-out.

The elevated temperature high cycle T-T test specimen fracture surface was very smooth with no fiber pull-out, while the elevated temperature low cycle T-T fatigue test specimen fracture surface was very rough with a lot of fiber pull-out, matrix cracking, and interface debonding.

The room temperature high cycle T-C test specimen fracture surface was slightly smooth with some fill and warp fiber pull out, while the room temperature low cycle T-C test specimen fracture surface was very rough with a lot of fill and warp fiber pull out; which was similar to the room temperature monotonic compressive test.

The elevated temperature high cycle T-C fatigue test specimen fracture surface was slightly smooth with transverse and through the thickness matrix cracking and no

noticeable fiber pull out; while the elevated temperature T-C low cycle fatigue test specimen fracture surface was smoother with some 90° fiber pull-out (similar to the elevated temperature monotonic tensile test).

MONOTONIC AND FATIGUE BEHAVIOR OF 2-D WOVEN CERAMIC MATRIX COMPOSITE AT ROOM AND ELEVATED TEMPERATURES (BLACKGLAS/NEXTEL 312)

1. Introduction

1.1. Background

Composites consist of one or more phases on a macroscopic scale whose mechanical performance and properties are designed to be superior to those of the constituent material acting independently. One of the phases is usually continuous and is called the matrix. The discontinuous phase is normally called the reinforcement, which is usually stiffer and stronger. Fiber reinforced composite materials are a very important class of composites to which the ceramic matrix composites (CMC) belong. Fiber reinforcement may be either non-woven such as in a cross ply or a unidirectional ply; or woven fabric (WF), which consist of interlaced fabric reinforcement layers. Woven fabrics are easier to handle (ensures low cost and automated fabrication), conform to complex shapes, provide better impact resistance, and exhibit larger damage tolerance than non-woven materials [1].

Ceramic matrix composites hold a tremendous potential for high temperature applications such as internal combustion engines, gas turbines, exhaust nozzles, space vehicles, and electronics because of their ability to withstand high temperatures, corrosion resistance, and foreign object damage tolerance. On the other hand, CMCs have weaknesses such as low fracture toughness, and low failure strain.

The brittle nature of ceramics promotes the tendency of any crack or flaw leading to catastrophic failure due to stress concentration at the crack tip. This tendency to catastrophic failure is inhibited through the use of fiber reinforcement. With the fibers being strong and the fiber-matrix interfacial bonds being relatively weak, the fiber debonding in close proximity to the crack tip permits the fibers to carry loads through the crack. This prevents a matrix crack from resulting in a catastrophic failure and permits a composite ultimate strength well beyond the matrix failure strain.

One of the most promising applications of woven CMCs is an exhaust nozzle for the next generation turbine engines. This application would take advantage of the compressive strength and high capability of CMCs. However, there are several problems with incorporating advanced materials into actual working components. These problems include issues like high cost and little data on mechanical behavior.

The composite investigated in this study was a 2-D woven fabric ceramic matrix composite (Blackglas/Nextel Nitrided 312). This material was manufactured by Lockheed using a low cost manufacturing procedure. There is little data concerning this CMC, as discussed in chapter 2.

1.2. Purpose

The purpose of this study was to investigate the monotonic and fatigue behavior of Blackglas/Nextel nitrided 312 at room temperature and at elevated temperature. Specifically, the study had three objectives: (1) to determine the material characteristics under monotonic tensile and compressive loading at room temperature and at elevated temperature (760°C), (2) to determine the relationship between maximum stress levels and number of cycles to failure under tension-tension and tension-compression low frequency (0.1 Hz) loading conditions at room and elevated temperatures, (3) to investigate the initiation and progression of damage under monotonic and fatigue loading conditions.

1.3. Approach

The composite investigated in this study was a 2-D woven fabric Blackglas/ Nextel nitrided 312. This material was manufactured by *Lockheed* using a low cost manufacturing procedure. Tests, in the present study, were conducted at room temperature and at elevated temperature (760°C). Tension-Tension (T-T) fatigue tests were accomplished using a minimum to maximum stress ratio of 0.05. Tension-Compression fatigue tests were accomplished using a minimum to maximum load ratio of -1. All fatigue tests were carried out at a frequency 0.1 Hz. Plots representing monotonic loading, maximum stress versus number of cycles and maximum & minimum strain versus number of cycles were obtained. Elastic modulus measurements were made from stress versus strain graphs using the initial linear loading portion of the graph. Scanning

electron microscopy was used to investigate the fracture surface of the material specimens to document the damage mechanisms and fracture modes.

The material specimens, as received, were about 152mm long, 12.3mm wide, and 2.3mm thick. The average cross section area ranged from 27 to 30mm^2. The specimens used for monotonic compression and (T-C) fatigue tests were cut to 11.43 cm long to minimize bending effects, while those used for monotonic tension, and (T-T) fatigue tests were cut to 12.7cm long for ease of handling. Chapter 2 describes the motivation for CMC development in general and previous research on Blackglas/Nextel 312 in particular. In Chapter 3, the test equipment, test procedure, and specimen details including preparation will be discussed. Chapter 4 presents and discusses the test results including the stress-strain curves, S-N curves, maximum & minimum strain versus number of cycles curves, and mechanisms of failure. Chapter 5 presents the conclusions and Chapter 6 presents some recommendations.

2. Background

While ceramic matrix composites (CMCs) in general are relatively new, several studies have nevertheless been completed describing their behavior under various loading conditions. Non-woven CMCs have received a lot of attention, and their behavior has been characterized and reported by several studies. On the other hand, less work has been done on woven CMCs, and their behavior needs to be investigated further. Since this study is focused towards woven CMCs, the following background will deal only with woven CMCs.

Groner [13] has studied the fatigue behavior of a 2-D woven fabric reinforced CMC (enhanced SiC/SiC) at elevated temperature (1100°C). He concluded that the presence of a notch had little effect on the fatigue life of this material, and most of the degradation had occurred in the first cycle.

Rodrigues, Rosa and Steen[1] reported on the fatigue behavior of a 2-D C_{fiber}/SiC_{matrix}. They reported difference in the tensile behavior of the material at room temperature and at 1200°C. They found that tensile & fatigue tests, at both room temperature and elevated temperature (1200°C), showed strain accumulation with number of cycles, and this accumulation was more pronounced at elevated temperature (greater than 0.5%). Scanning electron microscope (SEM) analysis of the as-received specimens in their study revealed that the matrix had microcracks perpendicular to each bundle. These microcracks were due to the large thermal expansion mismatch between the fibers

and the matrix. They also showed that monotonic and cyclic stress strain curves (σ-ϵ) at 1200°C did not show any significant difference.

Shuler, holmes and Wu [2] reported on the influence of loading frequency on the room temperature fatigue of a woven fiber /carbon matrix composite. They found that the fatigue life of the composite decreased as the loading frequency was increased. The frequency dependence of fatigue life was due, in part, to the accelerated rate of microstructural damage caused by internal heating that occured during the fatigue loading of the composite. Also, they attributed the fatigue damage to the non-uniform stress and strain distributions present in woven fiber architectures. The non-uniformity of the stress near the crossover points of fiber bundles lead to matrix cracking at these locations as the 0° bundles attempted to align with the tensile loading direction. Also delamination between plies occured by cracking.

Camus, Guillaumat and Baste [3] reported on the development of damage in a 2-D woven C/SiC composite under mechanical loading and showed that, under tensile loading, an extended non-linear stress-strain response was evident which related to a multi-stage development of damage involving transverse matrix microcracking, bundle/matrix and inter-bundle debonding as well as thermal residual stress release. In compression, after an initial stage involving closure of the thermal microcracks present from processing, the composite displayed a linear elastic behavior until failure.

Campbell and Gonczy [4] reported on the nitriding process and Blackglas^{TM} CMC properties. The results of their study indicated that a cost-effective process for the application of a boron nitride interface on a relatively low-cost fiber (Nextel^{tm} 312) is

possible using the ammonia containing gas, nitriding concept. They have shown that boron nitrite fiber interface can be formed in-situ on Nextel^{tm} 312 fibers by thermal treatment at temperatures above 1100°C in ammonia containing atmosphere. The interface coating serves as a compliant layer between the fiber and matrix to facilitate load transfer and crack deflection at the matrix/fiber interface leading to the non-catastrophic fibrous fracture mode of failure. In addition, the interface serves as a barrier between the matrix and the fiber preventing reactions between them that would lead to matrix/fiber debonding and the loss of fibrous fracture failure mode. Their study also showed that interfaces formed in a range of preferred conditions of temperature and time provided load transfer and fiber pull-out in ceramic fiber/ceramic matrix composites prepared with the Blackglas^{TM} preceramic polymer system. Composites with 3-point flexure strengths on the order of 200MPa with strains up to 0.4% and fibrous fracture failure were obtained.

Campbell and Gonczy [5] studied further the stability of nitrided Nextel^{tm} 312/ Blackglas^{TM} CMCs in air at temperatures between 600° and 800°C with an emphasis on the effect of oxidation on the room temperature mechanical properties and failure mechanisms. They reported excellent room temperature properties based on 3-point bend testing. Also, they have shown that Blackglas^{TM} composites fabricated with Nextel^{tm} 312 fabric in a 2-D configuration exhibited fibrous fracture (181MPa flexure strength and 0.4 % failure strain) at room temperature. After oxidation in the temperature range of 600°-800°C for times up to 100 hours, the composites retained fibrous fracture at room temperature with no sign of brittle failure. Oxidation at the higher temperatures and for

longer times produced higher failure strains (+50%), improved fiber pull-out, lower moduli (-50%), and slow, gradual reductions in flexure strength (-30%). In this study, they reported a modulus of 55.2GPa for the as-prepared specimen, and this value decreased with increasing temperature and oxidation times.

Vaidyanathan, Cannon, Tobin and Holmes [6] have also studied the effect of oxidation at 600°C for 20-1000 hours on the mechanical properties of Nextel ^{tm} 312/BN/ Blackglas ^{TM} composites. They reported that long-term oxidation was found to be detrimental on the tensile strength and modulus of the Nextel ^{tm} 312/BN/ Blackglas ^{TM} composite system. After oxidation for 96 hours the tensile properties were unchanged at room and elevated temperatures. The flexural strength of the Nextel ^{tm} 312/BN/ Blackglas ^{TM} composite system was relatively independent of the oxidation up to 111 hours; however an increasing strain to failure was observed. As the oxidation time increased, the fibrous nature of the fracture increased. For 500 hours oxidation, strength decreased by 50% relative to as-prepared composites. Their results indicated that oxidation beyond 200 hours may be embrittling the composite and may lead to possible weakening of the fiber/matrix interface due to oxidative degradation of the Blackglas ^{TM} matrix, reactions between the fiber and BN surface layer in presence of oxygen, or reactions between surface layer and Blackglas matrix. They reported an average tensile modulus of 66MPa for the as received specimen at 20°C and 566°C, and an average strain to failure of 0.415% at room temperature and 0.33% at 566°C. After oxidation for 96 hours at 20°C and at 566°C, the average tensile modulus dropped to

42GPa & 36GPa, respectively, and the average strain to failure was 0.33% & 0.44%, respectively.

Ranji, Sankar, and Kelkar [7] have reported on the mechanical properties of Nextell[tm]312 fiber reinforced SiC matrix composites in tension at room temperature. They showed that the Nextel/SiC composites had an average tensile strength of 112 ± 10MPa, with a smooth fracture surface. Fiber pull-out and fiber bridging were the major composite toughening factors. Very little microcracking was noticed, which may be because of a combination of factors such as fiber surface roughness, processing conditions and better thermal and elastic property matching after processing between the Nextel fibers and the SiC matrix.

Vidyanathan, Cannan, and Danforth [8] have studied the creep properties of pre-oxidized (600°C) specimens of Nextel[tm]312/BN/ Blackglas[TM] composites at 566°C and showed that the creep curve exhibited a large linear primary region (creep zone) and a flat steady state region, with a total creep strain of 0.25% after exposure to creep stresses (26 to 67MPa) for 850 hours. The primary creep region was believed to be due to fibers straightening out and load shifting to the fibers due to the effects of oxidation on the matrix.

Campbell, Gonczy, McNllan, and Cox [9] have studied the performance of Blackglas composites and reported little change in the oxidation behavior of Nextel[tm]312/BN/ Blackglas[TM] composites in the temperature range 500°C-700°C for times up to 4000 hours as a function of composite processing conditions. Also, they reported no improvement in oxidation behavior by altering the processing conditions of

Nextel^{tm} 312/BN/ Blackglas^{TM} composites if the application exposes the material at or above 600°C for extended periods of time.

Tobin, Holmes, Vaidyanathan, Cannon and Danforth [10] have reported on the effects of processing, oxidation and fiber architecture on thermal & mechanical properties of Nextel^{tm} 312/BN/ Blackglas^{TM} composites. They have shown that 100-hr pre-oxidation heat treatment at 600°C caused a 20-33% reduction in the ultimate strength as compared to the as-processed material; however the ultimate strain-to-failure was not strongly affected. Scanning electron microscope (SEM) observations of fiber pull-out suggested that pre-oxidation exposure increased fiber pull-out mechanisms. The effect of fiber architecture on the elevated temperature tensile properties of pre-oxidized Nextel^{tm} 312/BN/ Blackglas^{TM} composites was observed by a 33% reduction in strength for the quasi-isotropic architecture, as compared to the warp/weave fiber architecture. This was explained by the greater density of fibers available in the warp/weave configuration. Both of these architectures had a weak effect on the room-temperature compressive properties of this material. Also, the warp/weave & isotropic architectures had little effect on the shear properties. The shear strength was about 27MPa, and this suggested that the Blackglas matrix played a significant role in determining the interlaminar shear strength. Specimen thickness effect on room temperature tensile properties of pre-oxidized warp/weave Nextel^{tm} 312/BN/ Blackglas^{TM} composites was shown by a 20% reduction in tensile strength for specimens that were 1.6 mm thick, as compared to specimens 3 mm in thickness. The effect of test temperature on tensile behavior of air-exposed Nextel^{tm} 312/BN/ Blackglas^{TM} composites was not significant

10

from room temperature to 570°C, except a slight increase in strain to failure. This suggested that the initial reductions in tensile strengths tended to stabilize the tensile behavior over the room temperature to 570 °C range. The test temperature had little effect on the compressive properties of the material. At stress levels of 50MPa , there was an initial increase in creep strain (0.2%), after which the creep curve stabilized to a steady-state creep of 10^{-9} /hr.

Nejhad & Bayliss [11] reported on the mechanical properties of boron nitride coated Nextel ^{tm} 312/ Blackglas ^{TM} composite tubes which were manufactured using vacuum assisted resin transfer molding (VARTM) with & without injection pressure where the resin flows due to (a) gravity, (b) capillary effects, and (c) vacuum assistance. VARTM refers to the use of a vacuum pump to generate a vacuum in the flow front, thereby enhancing the part quality over the conventional RTM. They reported a failure stress of 150.82MPa & a modulus of 57.3GPa at room temperature, and a failure stress of 173.7MPa & a modulus of 41.56GPa at 600°C for Nextel ^{tm} 312/ Blackglas ^{TM} without injection pressure. Furthermore, a failure stress of 128.29MPa & a modulus of 36.93GPa at room temperature, and a failure stress of 145.45MPa & a modulus of 37.63GPa at 600°C for Nextel ^{tm} 312/ Blackglas ^{TM} with injection pressure using the C-Ring test. Extensive fibrous fracture was observed in all test specimens and fiber pull-out occured through the thickness. This study also reported that Nextel-reinforced composites had higher failure strength than Nicalon- reinforced composites due to a better performance of boron nitride coating over carbon coating and a higher performance of textile braided architecture.

Campbell, Leon, and McNallan [12] have reported on the effect of processing parameters on the surface nitridation of Nextel^{tm} 312 ceramic and showed that both temperature and time affected the thickness of the BN layer formed on the surface of Nextel^{tm} 312 specimens.

So far, most of the research done on Nextel^{tm} 312/ Blackglas^{TM} composites concentrated on the manufacturing process of this low cost new class of materials and the characterization of its monotonic & tensile fatigue behavior. Since, one of the possible applications of this material, which would take advantage of the compressive strength and high temperature capability of CMCs, is an exhaust nozzle for the next-generation turbine engines; it is necessary to investigate further the mechanical behavior of this material before it is put into use. This study will investigate the characteristic behavior of this material under tensile & compressive monotonic loads and tension-tension & tension compression fatigue loads at room & elevated temperatures.

3. Experimental Procedure

3.1. Test Material Description

The material tested was Nextel ^{TM} 312/Blackglas ^{TM} woven fabric ceramic matrix composite (CMC) and was supplied by Lockheed. The Nextel 312 is a polycrystalline metal oxide ceramic fiber. The reinforcement is made from *alumin-boria-silica* fibers, and has a composition of 62% Al_2O_3, 24% SiO_2, and 14% B_2O_3 w/o [11]. Nextel ^{TM} is white in color, has a fiber diameter of 10-12 microns, possesses desirable density and coefficient of thermal expansion, and is known for its thermomechanical qualities of retaining its strength at high temperatures for extended periods of time. The Nextel ^{TM} 312 material used in these tests had a *Boron Nitrite (BN)* interface coating.

The Blackglas ^{TM} system used as the matrix material in this study is a *preceramic siloxane polymer* system. Blackglas ^{TM} has the advantages of resistance to oxidation, low density, very low viscosity, controllable thermal expansion coefficient by varying the carbon content, short cure time (3 hours), no evolution of harmful reaction gases during the cure process, and ease & low cost of fabrication [11].

As received specimens were rectangular in shape and had an average length, width, and thickness of 152, 12.3, and 2.3mm, respectively. The cross-sectional area ranged from 27 to 30mm^2. Figure 3.1 is a schematic view of a test specimen, with the arrows showing the direction of loading.

13
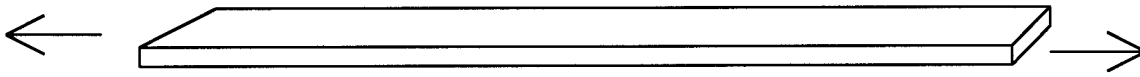
Figure 3.1 Test Specimen Schematic View

3.2. Specimen preparation

The specimens used for the monotonic compressive tests and tension-compression fatigue tests were cut to 11.43cm using an ISOMET low speed saw. This length was the shortest possible for ease of handling and short enough to alleviate flexure during testing. The specimens used for the monotonic tensile test and tension-tension fatigue tests were cut to 12.7mm also using an ISOMET low speed saw. Thermocouple wires were attached to the top and lower surfaces of the specimens to control the desired test temperature. These thermocouples were placed at 6.35mm from the center of the specimen. The idea behind these two thermocouples was to accurately measure the temperature on both sides of the specimens, so that uniform temperature distribution was obtained throughout the cross-section of the test specimens. After the specimens were cut to required length and the thermocouples were attached (in alleviated temperature tests), they were placed in the Material Test System and the test load was applied.

3.3. Test Equipment

A 22.4KN Material Test System (MTS) horizontal tensile tester, Figure 3.2, was used for the present study. The components of the test system were cooled using cold water provided by a Neslab model HX-75. Cooling water was circulated through the

MTS 647 hydraulic wedge grips. The cooling water also cooled the heat lamps and the

isolation block between the grip wedge assemblies and the model 661.20E-01 force

transducer. The heat lamps also had internal airflow to improve heat dissipation.
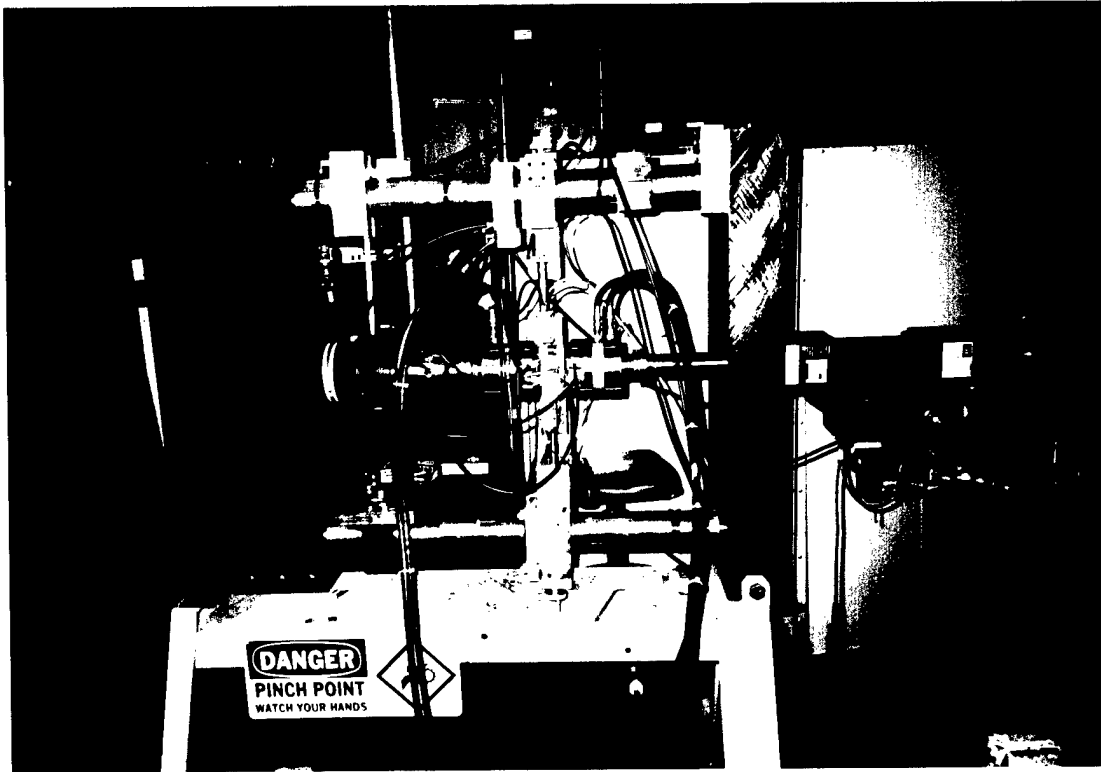
Figure 3.2 22.4KN Material Test System (MTS) horizontal tensile tester

The hydraulic grip wedge assemblies were operated by means of an MTS 685

hydraulic grip supply. Tensile, and compressive pressure was applied to the specimen

through a model 244.12 hydraulic actuator. Displacement of the test specimen was

measured using an MTS 632.52E-14 extensometer. The extensometer gauge length was

12.0 mm, and it was calibrated to display 0.02648 full scale displacement. Monitoring

and control functions were provided through an MTS model 458.2 microconsole, with

appropriate displacement, force, and strain plug-ins. Some feedback signals had to be

filtered, and this was done through a Rockland model 852 filter. Barbor-Colman 560 temperature controllers regulated the heat lamp assemblies to maintain the test section temperature at 760°C. The temperature controllers used feedback (temperature control) thermocouples mounted directly on the top and lower surfaces of the specimen. Both, monotonic and fatigue testing were accomplished using special software developed by Mark M. Derriso (previously structures/materials testing laboratory technician-Air Force Institute of Technology).

3.4. Test Station Alignment

The test equipment had to be aligned before any testing could be conducted. The alignment was necessary to ensure that only pure tensile or compressive loads would be transmitted to the specimen. Misalignment would cause bending and non-symmetrical axial loads and strains and, therefore, unreliable data. These non-axial loads could adversely affect the monotonic failure stresses and fatigue life of the specimen, causing premature failure.

Although test machine alignment was previously done by AFIT personnel, it was carried out again to make sure that it was still in alignment. Alignment was performed using MTS model 609, which was mounted on the test station between the load cell and the head block, an aluminum bar with eight strain gauges mounted in the grips of the test section. Monitoring of the aluminum block deformation was accomplished using alignment software and a micro-computer. The top grip alignment and rotation were adjusted until all strain gauges displayed less than 100μ strain variation [13].

The top and lower horizontal heat lamps were in good alignment with respect to the test specimen and produced an even distribution of temperature across the specimen working cross-section of $760 \pm 3°C$.

3.5. Test Procedure

The test procedure started by measuring the test specimen width and thickness, from which the cross-sectional area was calculated. After this, the specimen was cut to the required length for the test (11.43cm for the monotonic compression & tension-compression fatigue tests, and 12.7cm for the monotonic tension & tension-tension fatigue tests) using an ISOMET low speed saw. Thermocouples were installed directly on the top and lower surfaces of the test specimen for controlling the test temperature. These thermocouples were held in position using a 36 GA Chromel, and 903 HP High Strength (1600°C) Alumina Adhesive. After this, the specimen was mounted in the left hand side grip (fixed). It was made sure that about 3.81cm of the specimen was inside the grip assembly before gripping. After gripping this side using the MTS 685 hydraulic grip supply, the right hand grip was moved slowly and carefully towards the specimen until about 3.81cm of the specimen was inside the grip assembly, then the control on the MTS 458.20 microconsole was changed from displacement to load control and the right hand side of the specimen was gripped using the MTS 685 hydraulic grip supply. The upper & lower limits of the displacement & load on the MTS 458.20 microconsole were set to the desired values depending on the test type. After the specimen was gripped, the extensometer was moved to touch the specimen edge and its opening was adjusted to display a strain reading of as close to zero as possible on the

MTS 458.20 microconsole (less than 0.00002). After this, the heat lamps were placed as close to the specimen as possible from the upper and lower sides (approximately 6.35mm from the specimen).

Depending on the test type, monotonic or fatigue, test software was chosen, and the relevant test parameters (cross-sectional area, test temperature, maximum stress required, strain card, load card, frequency, thermostrain, Dac interval, maximum to minimum stress-ratio "R- value") were entered. The elevated test temperature was allowed to stabilize at 760°C before starting the test. The test was then started through the microcomputer, and the span of the load control was then turned to maximum. The specimens that broke under testing were cut 6.35mm from the failure surface and gold coated using the SPI-MODULE ^{TM} SPUTTER COATER, and SEM photographs were taken, so that analysis of fracture mechanisms could be made in order to understand the behavior of this material under the loading conditions investigated.

4. Results and Discussion

The main purpose of this study was: (1) to determine the material characteristics under monotonic tensile and compressive loads at room temperature and at elevated temperature (760°C), (2) to determine the relationship between maximum stress levels and number of cycles to failure under tension-tension (T-T) and tension-compression (T-T) low frequency (0.1 Hz) loading conditions at room and elevated temperatures, (3) to investigate the initiation and progression of damage mechanisms and failure modes under monotonic and fatigue loading conditions. The loading waveform in the fatigue tests corresponded to a triangular wave with a frequency of 0.1 Hz. The ratio of minimum to maximum stress levels ($\sigma_{min}/\sigma_{max}$), called R-ratio, in the T-T and T-C fatigue tests was 0.05 & -1, respectively. σ_{min} is the smallest positive stress for T-T tests or the magnitude of the largest negative stress for T-C tests. σ_{max} is the largest positive stress for both T-T and T-C tests.

Section 1 of this chapter discusses the monotonic tests. Section 2 discusses the T-T fatigue tests, and section 3 discusses the T-C fatigue tests. Section 4 presents the S-N curves and discusses the fatigue life of the material. Section 5 presents minimum & maximum strain of the test specimens during fatigue tests. Section 6 discusses the damage mechanisms in the test specimens.

Table 4.1 shows all the tests conducted in this study. This table includes type of test, specimen identity, test temperature, maximum stress, and number of cycles to failure. The number of cycles to failure for monotonic tests was taken as one cycle.

19

Duplicate tests could not be conducted due to the limited number of material specimens available.

Table 4.1. Summary of Tests

Test Type	Specimen I.D	Test Temperature	Max. Stress (MPa)	Cycles
Monotonic Tension	10-14	Room Temperature	69.24	1
Monotonic Tension	10-1	760°C	65.22	1
Monotonic Tension	9-8	760°C	69.28	1
Monotonic Tension	9-9	760°C	62.99	1
Monotonic Compression	10-9	Room Temperature	273.91	1
Monotonic Compression	9-7	760°C	334.48	1
Tension-Tension Fatigue	9-14	Room Temperature	40	40,000
Tension-Tension Fatigue	9-15	Room Temperature	45	40,000
Tension-Tension Fatigue	19-1	Room Temperature	50	10,922
Tension-Tension Fatigue	19-2	Room Temperature	52.5	11,310
Monotonic Compression	19-3	Room Temperature	55	1618
Tension-Tension Fatigue	20-6	760°C	20	30,427
Tension-Tension Fatigue	10-12	760°C	25	15,545
Tension-Tension Fatigue	10-11	760°C	30	15,710
Tension-Tension Fatigue	10-10	760°C	40	2,210
Tension-Comp. Fatigue	9-5	Room Temperature	30	40,000
Tension-Comp. Fatigue	9-6	Room Temperature	35	40,000
Tension-Comp. Fatigue	9-4	Room Temperature	40	11,069
Tension-Comp. Fatigue	9-13	Room Temperature	45	162
Tension-Comp. Fatigue	9-12	760°C	20	40,000
Tension-Comp. Fatigue	20-13	760°C	25	16,086
Tension-Comp. Fatigue	20-11	760°C	30	10,315
Tension-Comp. Fatigue	20-9	760°C	40	1,407

4.1. Monotonic tests

4.1.1. Room Temperature Monotonic Tensile Test

This test was conducted at room temperature (20°C). The specimen was loaded under tension until it broke. Figure 4.1 shows the stress-strain curve.
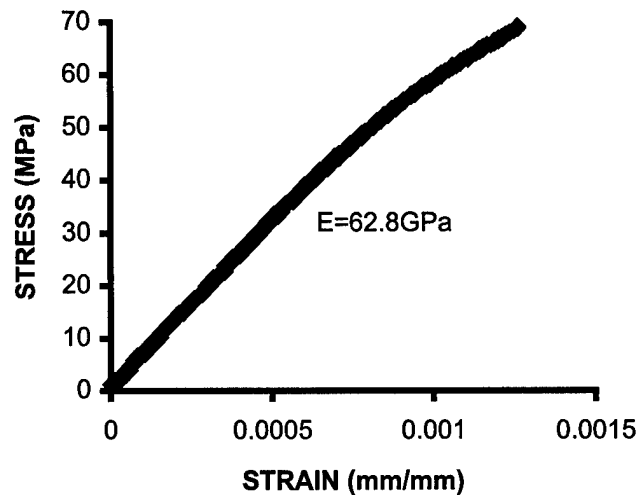
Figure 4.1 Room Temperature Monotonic Tensile Test

This graph shows a linear stress-strain relationship from the onset of loading up to about 44MPa stress level, after which the relation became nonlinear until the specimen broke at a maximum stress of 69.4MPa, and a maximum strain of 0.1261%. The Young's modulus is the slope of the initial linear region of the stress-strain curve and is found to be 62.8GPa.

4.1.2. Elevated Temperature Monotonic Tensile Test

This test was carried out at 760°C. The temperature was allowed to stabilize for more than 15 minutes before the test was started. The specimen was loaded until it failed. Figure 4.2 shows the stress-strain relationship for this test.
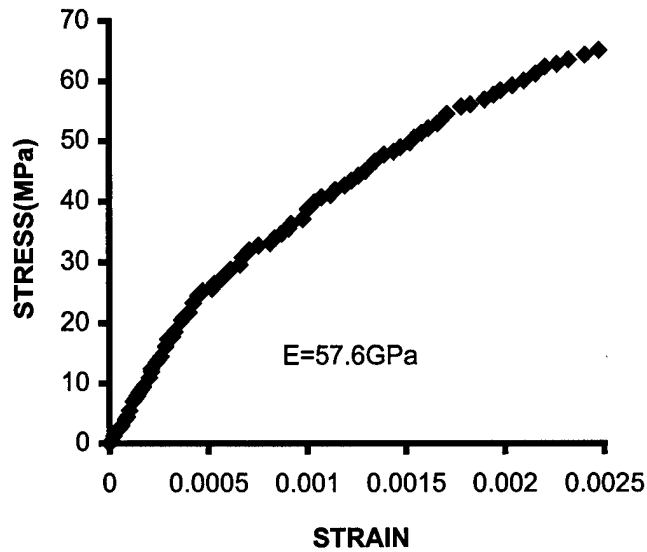
Figure 4.2 Elevated Temperature Monotonic Tensile Test

It can be seen that the stress-strain relationship is linear up to about 24MPa, which is the proportional limit, then the curve becomes non-linear and shows a lower slope. The Young's modulus of elasticity calculated from the linear region up to the proportional limit is 57.6GPa, and the slope in the non-linear region is 23.2GPa. This is an indication that damage had occured in the specimen. The damage mechanisms will be discussed in section 6 of this chapter. The failure stress in this test was 65.2MPa, which is slightly lower than the room temperature value. The failure strain was 0.2474%, which is about twice as much as the room temperature test failure strain. These values of failure stress & failure strain indicate that the elevated temperature has little effect on the maximum stress the material can withstand before it fails, and the material can withstand higher values of strain before it fails under elevated temperature conditions.

4.1.3. Room Temperature Monotonic Compression Test

This test was performed at room temperature. The specimen was loaded in compression until failure. The test specimen had been cut to a short length (about 11.43cm) to alleviate non-axial loads that would have adversely affected the test results. Figure 4.3 shows the stress-strain relationship for this test. It can be seen that the stress-strain relationship remained linear until failure, which occured at a stress level of 273.9MPa. The failure strain was 0.43%. The Young's modulus of elasticity obtained from this test is 62.5GPa.
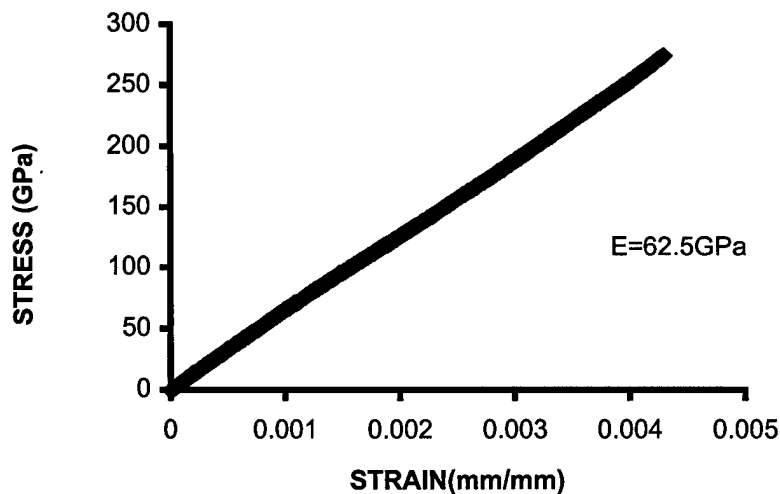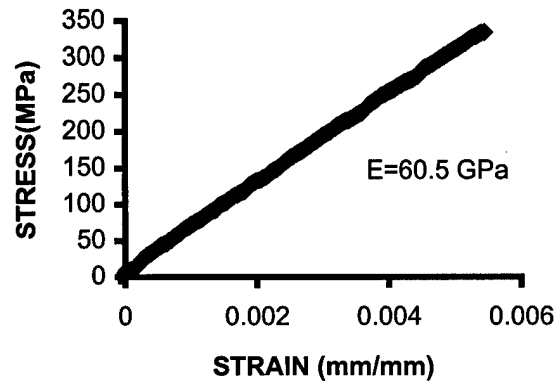

Figure 4.3 Room Temperature Monotonic Compression Test

4.1.4. Elevated Temperature Monotonic Compression Test

This test was carried out at 760°C. Figure 4.4 Shows the stress-strain relationship

for this test.

Figure 4.4 Elevated Temperature Monotonic Compression Test

The stress-strain relationship as can be seen from the above graph is linear up to

failure. The maximum compressive stress at failure was 334.5MPa, and the failure strain

was 0.5446%. The Young's modulus of elasticity obtained from this test is 60.5GPa.

Simple comparison between the room & elevated temperatures tests shows that

the failure stress at room temperature is about 18% lower than that at the elevated

temperature, and the failure strain at room temperature is about 21% lower than that at the

elevated temperature.

Table 4.2 shows the monotonic tests conducted, the maximum stress & maximum

strain at failure, the proportional limit (PL), and the Young's modulus of elasticity

obtained from these tests. It is clear that the values of Young's modulus of elasticity

obtained from the monotonic tension & compression tests at room temperature and at elevated temperature agree with each other. The room temperature values for Young's modulus lie within 5% of previously established values [6], and the elevated temperature values lie within 12% of these values [6]. The stress-strain curves become non-linear beyond the proportional limit as damage takes place progressively in the inter-yarn region, 90° fibers, matrix, and 0 ° fibers as mentioned in chapter 2. Also, in all of these tests the fracture occured perpendicular to the uniaxial load.

Table 4.2. Summary Of Maximum Stress, Strain, Young's Modulus, and Proportional Limit

| Test Type	Max.Stress (MPa)	Max.Strain (%)	E (GPa)	PL(MPa
Room Temperature Tension	69.4	0.1261	62.8	44
Elevated Temperature Tension	65.2	0.2474	57.6	24
Room Temp. Compression	273.9	0.43	62.5	273.9
Elevated Temp. Compression	334.5	0.5446	60.5	334.5

4.2. Tension-Tension Fatigue Tests

Tension-Tension fatigue tests were carried out at room and elevated temperatures. All these test were carried out at an R-Ratio of 0.05 and a frequency of 0.1Hz.

4.2.1. Room Temperature T-T Fatigue Tests

These tests were carried out at room temperature in normal laboratory conditions. The first test was started at a maximum stress level of 40MPa (about 60% of RT failure stress). The specimen survived 40,000 cycles and did not break. This number of cycles was considered as cycle run-out. The test was stopped at this number of cycles. The second test was at 45MPa maximum stress, and the specimen also survived 40,000 cycles and did not break. The third fatigue test was carried out at 50MPa maximum stress level. The specimen survived 10,922 cycles at this stress level. Two more tests were carried out at 52.5 and 55MPa maximum stress levels. The specimens survived 11,310 & 1,618 cycles at these two stress levels respectively. Figure 4.5 shows the S-N curve for these tests.
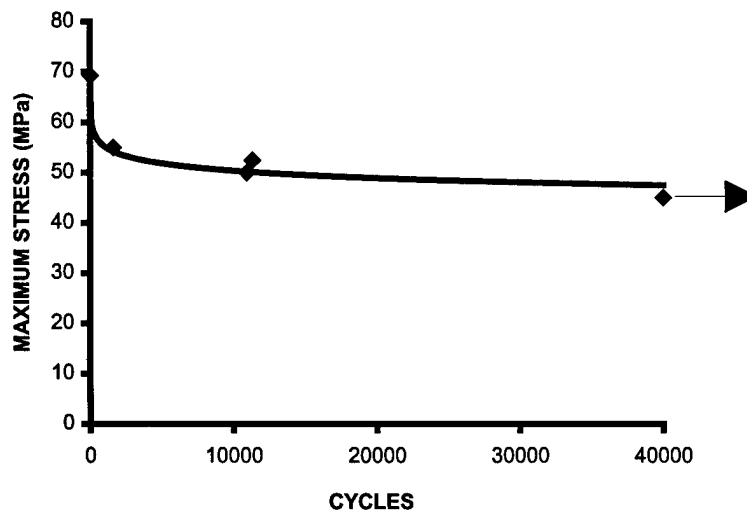
Figure 4.5 Room Temperature Tension-Tension Fatigue Test S-N Curve

4.2.2. Elevated Temperature T-T Fatigue Tests

These tests were carried out at 760°C under normal laboratory conditions. The first test was carried out at 20MPa (about 40% of elevated temperature failure stress). The specimen survived 40,000 cycles and did not break. Three more fatigue tests were carried out at maximum stress levels of 25, 30, and 40MPa. The number of cycles to failure at these maximum stress levels was 15545, 15710, and 2210, respectively. Figure 4.6 shows the S-N curve for these tests.
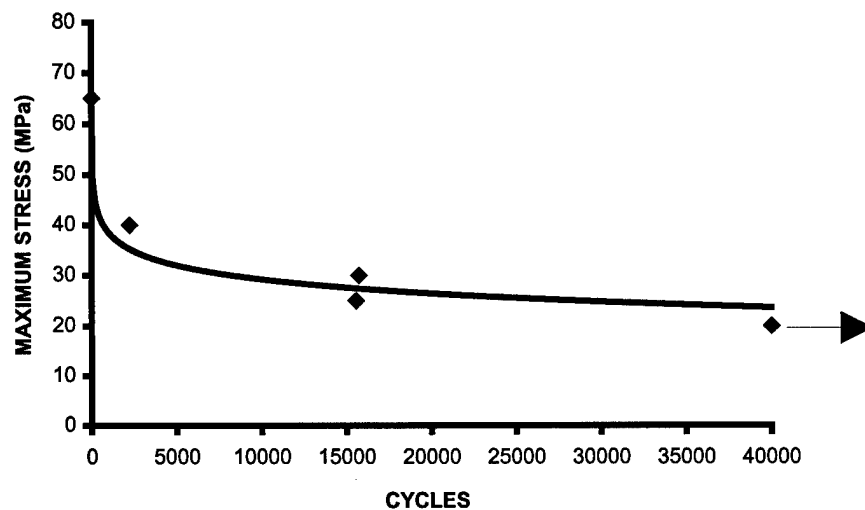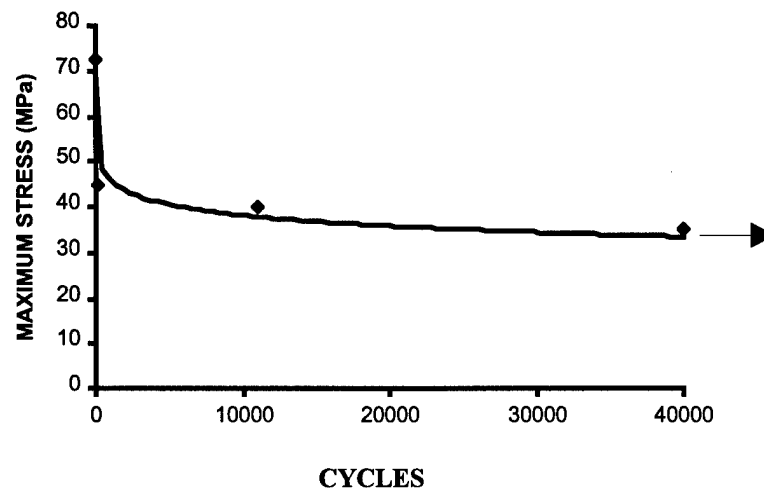

Figure 4.6 Elevated Temperature Tension-Tension Fatigue Tests S-N Curve

4.3. Tension-Compression Fatigue Tests

Tension-Compression fatigue tests were carried out at room and elevated temperatures. All these tests were carried out at an R-ratio of -1, and a frequency of 0.1Hz.

27

4.3.1. Room Temperature T-C Fatigue Tests

These tests were carried out at room temperature in the ambient laboratory conditions. The first test was carried out at 30MPa maximum stress level. The specimen did not break at this stress level and survived the 40,000 cycle run-out. The second test was at 35MPa, and the specimen did not break at this stress level either. Two more tests were carried out at 40 & 45MPa maximum stress levels. The number of cycles to failure at these maximum stress levels were 11069 and 162, respectively. Figure 4.7 shows the S-N curve for these tests.
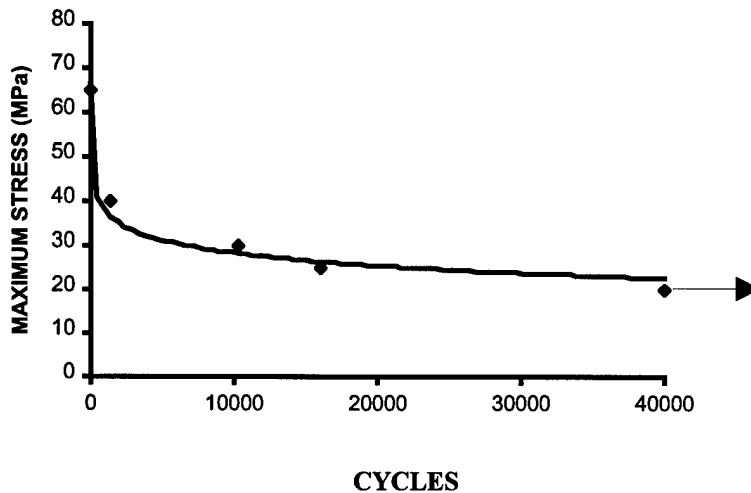

Figure 4.7 Room Temperature Tension-Compression Fatigue Tests S-N Curve

4.3.2. Elevated Temperature T-C fatigue Tests

These tests were carried out at 760°C under normal laboratory condition at a frequency of 0.1Hz. The first test was carried out at 20MPa maximum stress level. Run-

28

out cycles were exceeded at this stress level and the specimen did not break. Three more tests of this kind were conducted at 25, 30, and 40MPa maximum stress level, and the number of cycles to failure was 16086, 10315, and 1407, respectively. Figure 4.8 shows the S-N curve for these tests.

Figure 4.8 Elevated Temperature Tension-Compression Fatigue Tests S-N Curve

4.4. S-N Curves: Comparison

Figure 4.9 shows the S-N curves for all fatigue tests combined on one graph for comparison purposes. This is shown on regular scale. Figure 4.10 shows these curves using a logarithmic scale on the x-axis (number of fatigue cycles). These graphs include the monotonic tensile strengths at room and elevated temperatures as data points corresponding to one cycle to failure.

The S-N curves clearly illustrate the dependance of fatigue life on the maximum applied stress level. In the room temperature T-T fatigue curve, there is a sharp decrease in the number of cycles to failure at stress levels above 54MPa (78% of failure stress),

29

and the number of cycles to failure becomes almost independent of stress levels below 50MPa (72% of failure stress). The sharp decrease in the number of cycles to failure at high stress levels is also evident in the T-T elevated temperature tests. The fatigue life increases noticeably as stress levels drop below 36MPa (55% of failure stress) until 24MPa stress level (38% of failure stress), below which the material may have infinite life. The fatigue strength for 40,000 cycles at room and elevated temperatures under tension-tension fatigue are 48MPa & 24MPa, respectively.

In the room temperature T-C tests, the sharp decrease in fatigue life starts at about 45MPa (64% of failure stress). At stress levels below 45MPa, the fatigue life increases as the stress level drops down to 36MPa below which the fatigue life becomes infinite. In the elevated temperature T-C fatigue tests, the sharp decrease in fatigue life is noticed at stress levels above 30MPa (46% of failure stress). Below 30MPa stress level the fatigue life increases with lowering stress until 25MPa stress level, below which the number of cycles to failure becomes infinite.

At room temperature there is a significant difference between T-T & T-C fatigue life of the material under investigation. The number of cycles to failure at a given stress level in T-T is higher than in T-C, and the material can withstand higher maximum stress levels in T-T than in T-C. At the elevated temperature, it can be seen that there is practically no difference between T-T & T-C fatigue tests, and the material behaved almost exactly the same. In both T-T & T-C fatigue tests, the material can withstand higher maximum stress levels at room temperature than at the elevated temperature, indicating that more damage occured in the material due to the elevated temperature.
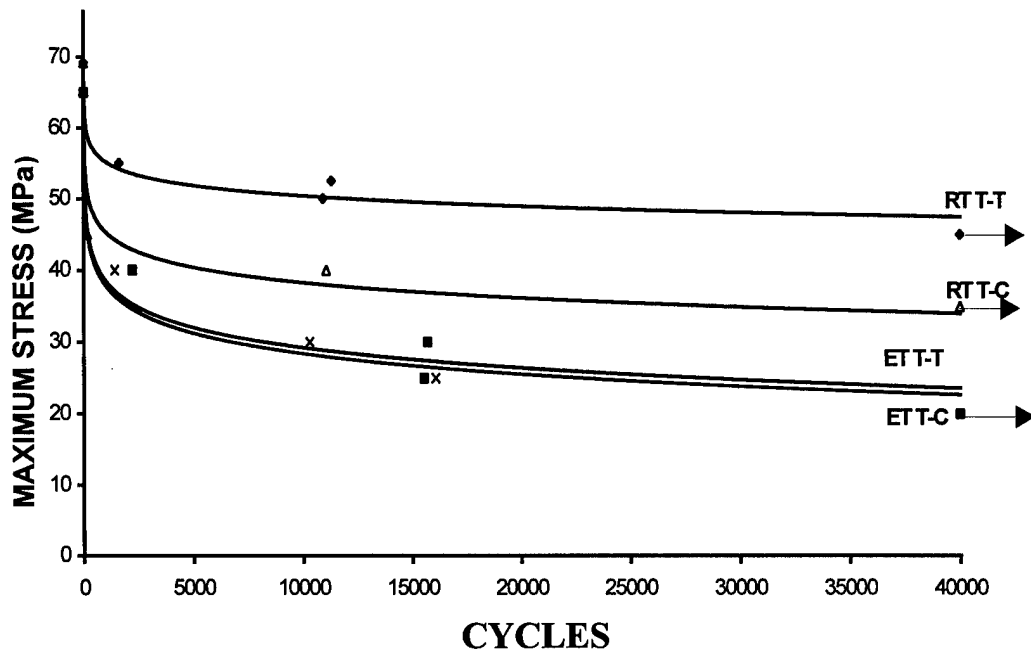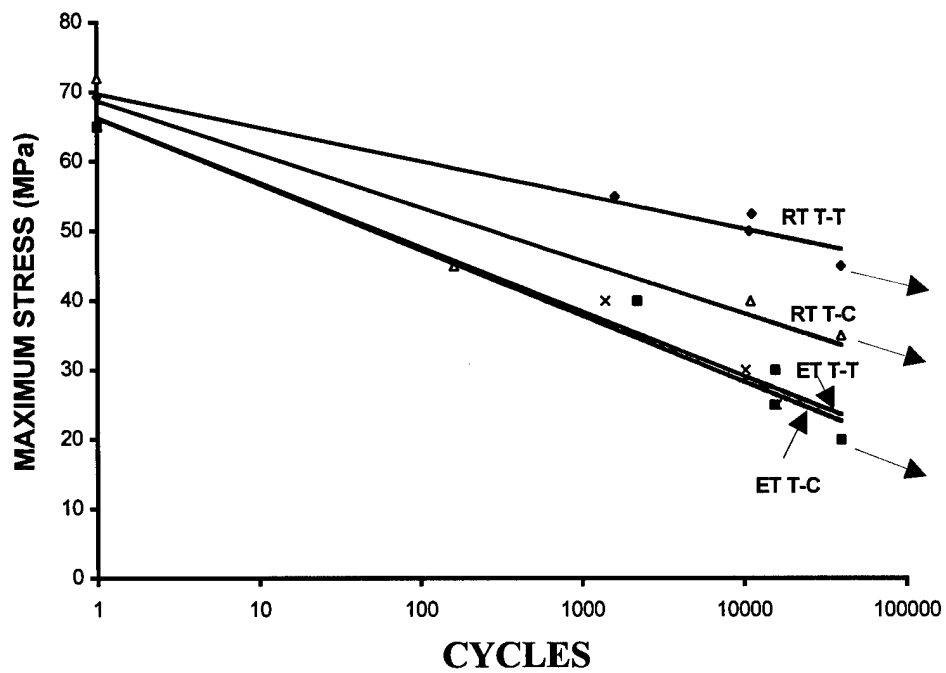
Figure 4.9 S-N Curves


Figure 4.10 S-N Curves

31

The fatigue strength for 40,000 cycles at room temperature for the T-T fatigue tests is about 48MPa compared to 36MPa for the T-C fatigue tests. The corresponding value at the elevated temperature is about 24MPa for both T-T & T-C fatigue tests. So, the fatigue strength for 40,000 cycles is highest for the room temperature T-T fatigue tests, followed by the room temperature T-C fatigue tests, and lowest for the elevated temperature T-T & T-C tests.

The S-N curves in logarithmic scale show inverse linear relationships between maximum stress levels & cycles to failure with the RT T-T fatigue tests giving the highest number of cycles to failure, followed by the RT T-C fatigue tests. The elevated temperature fatigue tests survived the lowest number of cycles at a given maximum stress level. The RT T-T S-N curve is the most flat amongst these tests, followed by the RT T-C, and the elevated temperature T-T & T-C which overlap showing that there is practically no significant difference in the fatigue life of the material being tested under T-T & T-C fatigue loading at the elevated temperature. These curves clearly indicate that, at a given maximum stress level, the fatigue life of the material is lower at the elevated temperature than that at room temperature. The maximum stress level at which cycle run-out is achieved is about 24MPa lower at the elevated temperature than that at the room temperature, in the T-T tests, and 12MPa in the T-C tests.

4.5. Maximum and Minimum Strain

Maximum and minimum strains were monitored during fatigue tests. Figures 4.11, 4.12, 4.13, and 4.14 present the typical data on strain accumulation during fatigue

testing of the specimens under room temperature T-T & T-C and elevated temperature

T-T&T-C. All strains discussed in this section are mechanical strains only. Thermal strain

has been removed by subtracting it from total strain at the beginning of the test to give
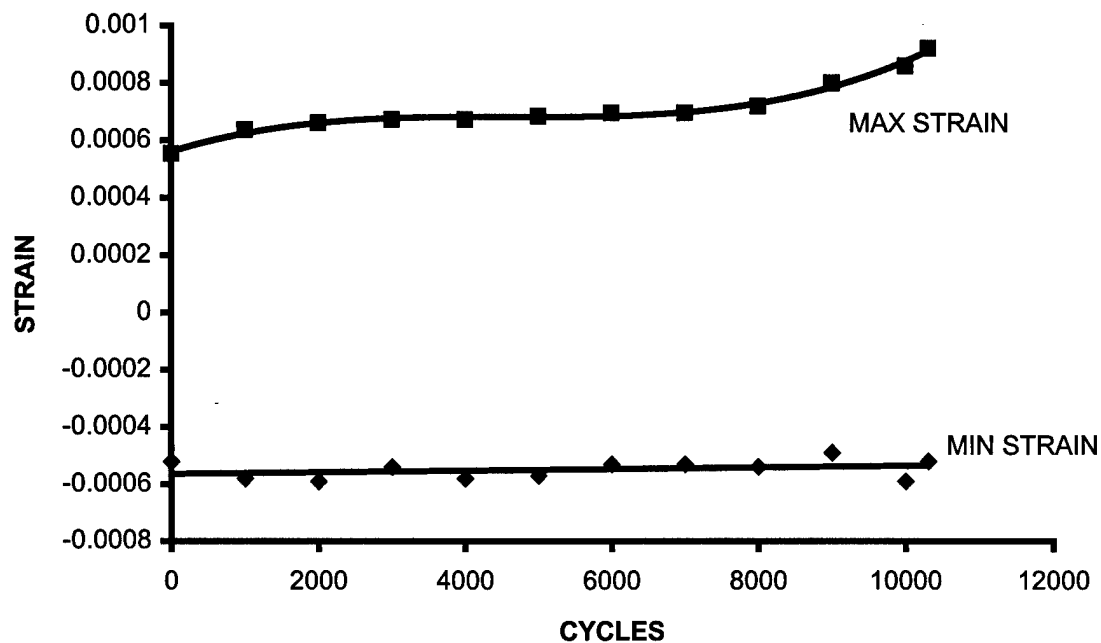
mechanical strain, which is the quantity of interest.
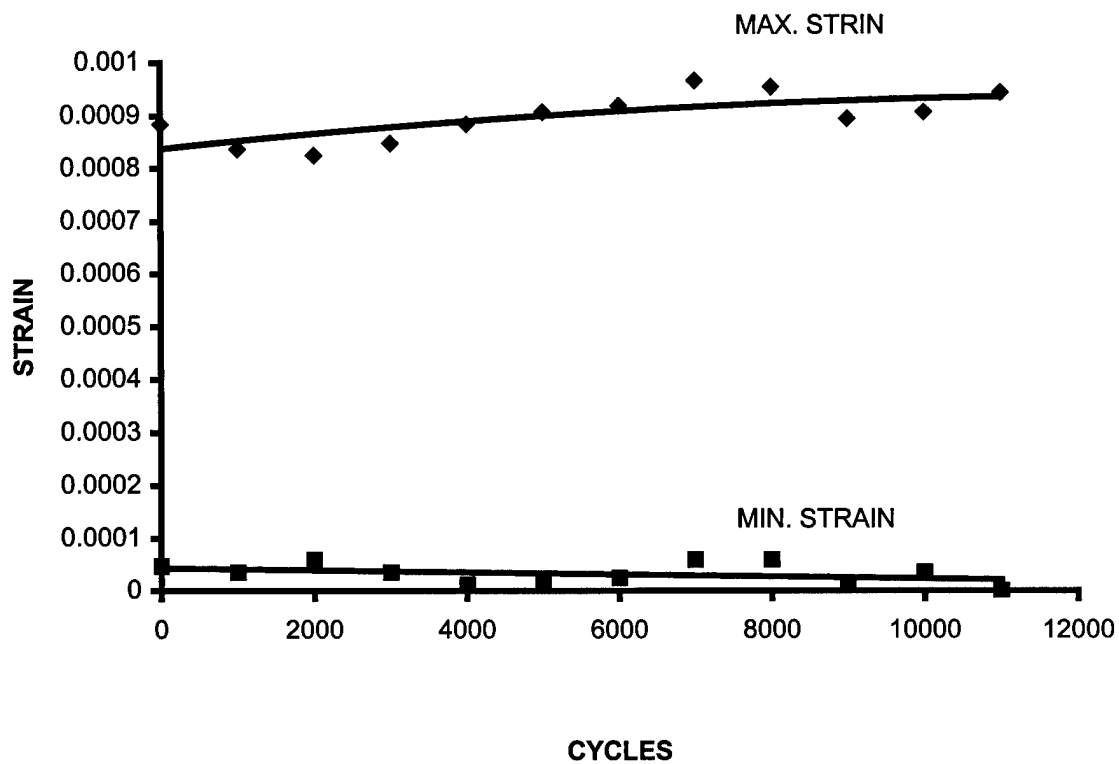
Figure 4.11 52.5MPa Room Temperature Tension-Tension
Fatigue Test Min.and Max. Strain
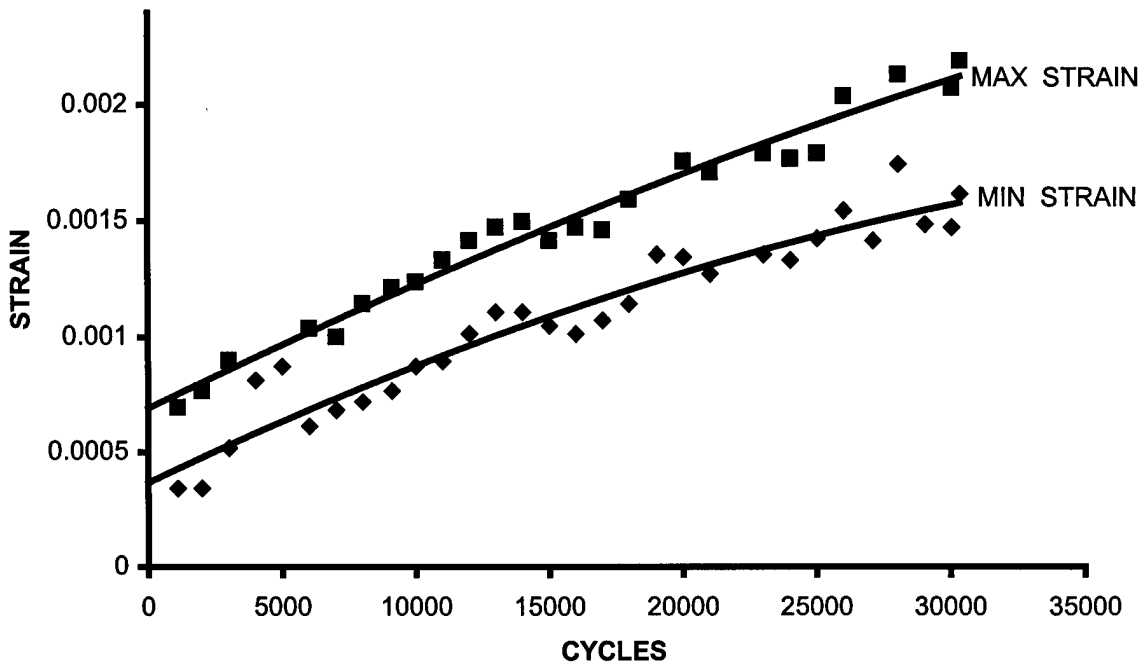
Figure 4.12 20MPa Elevated Temperature Tension-Tension
Fatigue Test Min. and Max. Strain
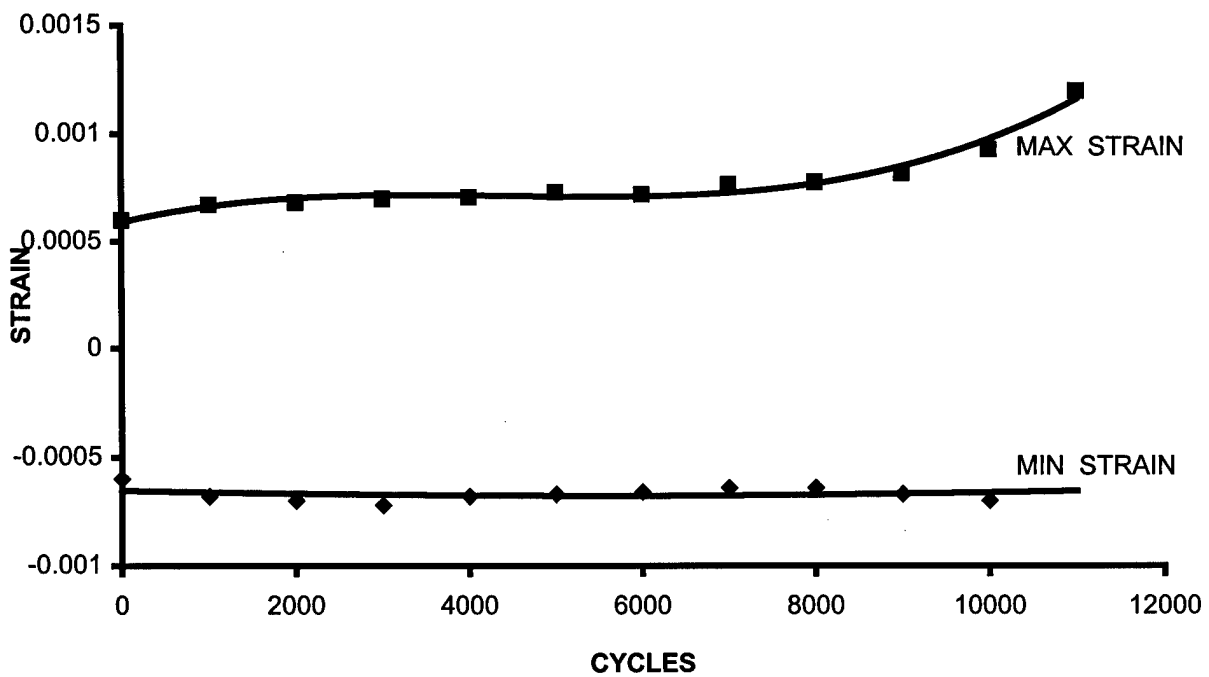
Figure 4.13 30MPa Room Temperature Tension-Compression
Fatigue Test Min. and Max. Strain

Figure 4.14 30MPa Elevated Temperature Tension-Compression
Fatigue Test Min. and Max. Strain

Figure 4.11 shows the values of minimum and maximum strains for the 52.5MPa

maximum stress room temperature tension-tension fatigue test. It can be seen clearly that

there is no significant variation in both, minimum and maximum strain values from the

onset of cycling until failure. The minimum strain is about 0.0035%, and the maximum

strain is about 0.09%. These values of strain indicate that only little damage has occured

to the specimen in the first cycle, and much less damage occured in the subsequent cycles

up to failure. Figure 4.11 shows no signs of creep. This phenomena was also observed in

the 55MPa room temperature tension-tension fatigue test with slightly higher minimum

and maximum strains.

Figure 4.12 shows the minimum and maximum strain obtained from the 20MPa elevated temperature tension-tension fatigue test. The minimum and maximum strains started at about 0.03% & 0.06 %, respectively; and then both of these strains increased as the number of cycles progressed, up to failure. The rate at which these strains increased became higher as the failure cycle was approached. The difference between the minimum and maximum strains remained almost constant until near failure, where the difference increased slightly up to failure. This accumulation of strain indicates that the deformation mechanism seen by the specimen during most of cycling is predominantly from creep. The increased strain also corresponds to stiffness reduction. This phenomenon was also seen at higher maximum stress levels of the elevated temperature tension-tension fatigue tests with greater difference between minimum and maximum strain, and the rate at which the strain increases is higher at these higher maximum stress levels.

Figure 4.13 shows the maximum and minimum strains obtained from the 30MPa room temperature tension-compression fatigue test. The minimum strain, which is about (-0.065%) remained constant from the beginning of the test up to failure. The maximum strain, also remained constant (about 0.07%) up to about 75% of the fatigue life of this test after which it increased with number of cycles until it reached 0.12% at failure. In this test, damage occured to the specimen, but no creep was present.

Figure 4.14 shows the 30MPa elevated temperature tension-compression fatigue test minimum and maximum strain. The minimum strain did not vary considerably and remained constant at about -0.055%. The maximum strain also remained constant at about 0.06% until about 75% of the fatigue life of this test, after which it increased with

number of cycles until it reached 0.09% at failure. In this test, damage occured to the specimen, but no creep was present.

So, it is clearly seen, that the elevated temperature has no significant effect on the strain behavior of the material under investigation when it is subjected to tensile-compressive fatigue loads. No sign of strain accumulation is noticed up to about 75% of the fatigue life of the specimen. After this value, the maximum strain slightly increases with cycle progression until failure is achieved. On the other hand, a big difference exists in the strain behavior of the material when it is subjected to tension-tension fatigue loads at room and elevated temperatures. While at room temperature tension-tension fatigue loads, both minimum and maximum strains remain almost constant up to failure; these strains, under elevated temperature, increase at the same rate as the number of fatigue cycles increase up to failure with the difference between them remaining almost constant, indicating that creep has occurred in the test specimen under elevated temperature tension-tension fatigue loading conditions. This is an indication of progressive microstructural damage in the form of matrix cracking, matrix/fiber interface debonding and fiber pull-out until failure. These failure mechanisms will be discussed in the next section.
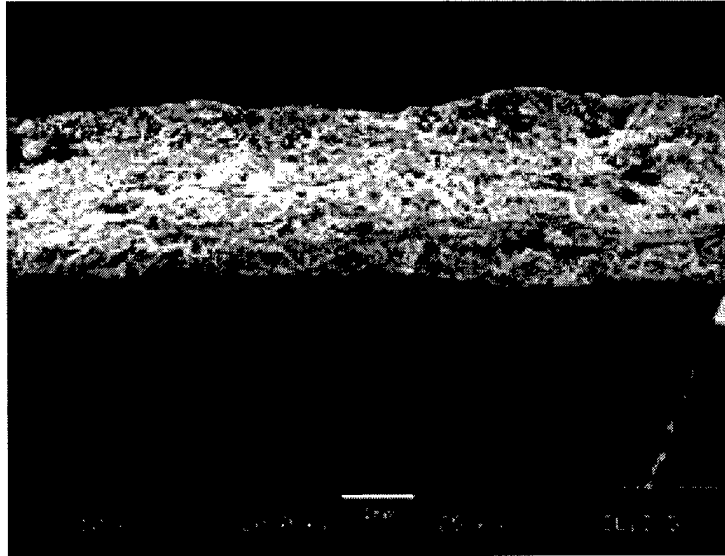
4.6. Damage Mechanisms
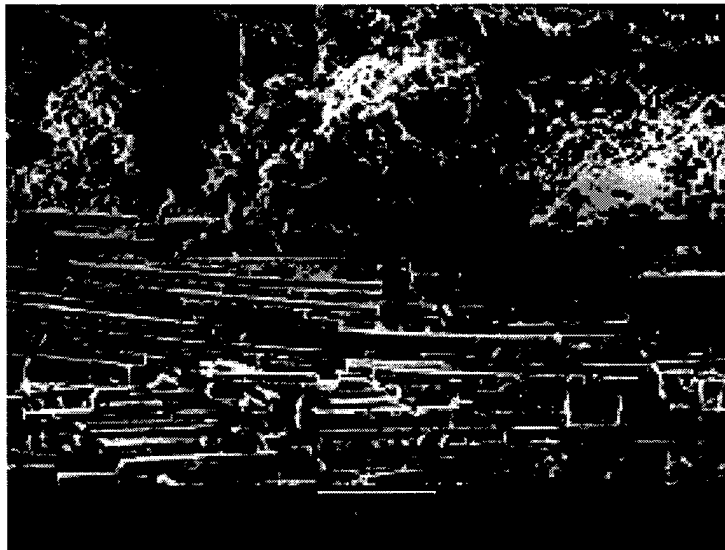
4.6.1. Monotonic Tensile Tests

An overview of the magnified fracture surface of the room temperature monotonic tensile test is shown in Figure 4.15. Scanning Electron Micrographs of the room temperature test specimen fracture surface are shown in Figures 4.16-4.18. The fracture surface edges, as can be seen in Figure 4.15 and Figure 4.16, are relatively smooth with some roughness at some locations. Matrix cracking is visible in Figure 4.17. The 90° yarn fiber bundles in the center and left hand side of Figure 4.17 display yarn splitting and some degree of fiber pull-out as well as evidence of matrix cracking, interface debonding, and fiber breakage. Figure 4.18 displays clearly, more debonded 90° yarn fibers throughout the fractured surface. This phenomena, along with matrix cracking, interface debonding, and fiber breakage may have started at the pores and grew in the 90° direction and in the thickness direction of the specimen. The overall fracture surface, as it can be seen from Figure 4.18, is relatively smooth with some 90° fiber pull-out.
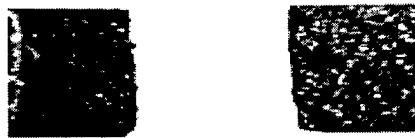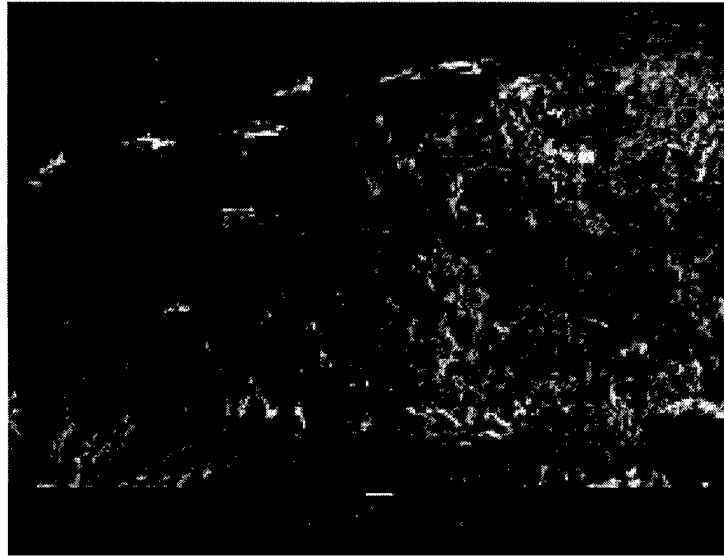

Figure 4.15 Room Temperature Monotonic Tensile Test Surface, Top View

38

Figure 4.16 Room Temp. Monotonic Tension Test Fracture Surface SEM, 12X

Figure 4.17 Room Temp. Monotonic Tension Test Fracture Surface SEM, 200X
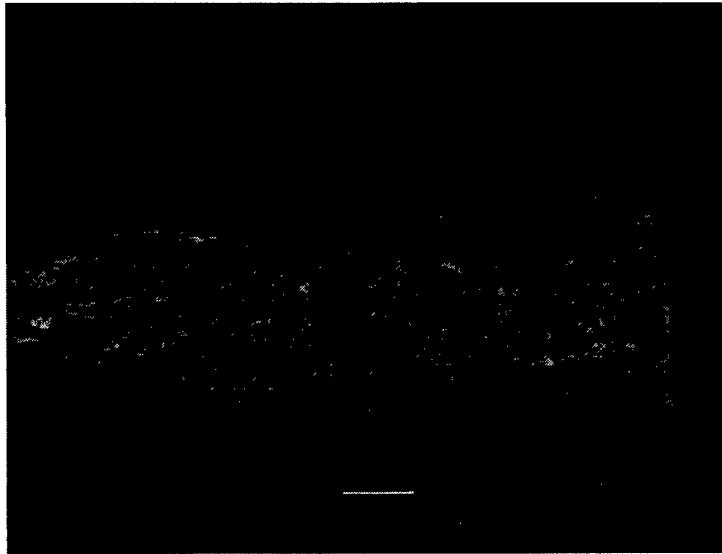
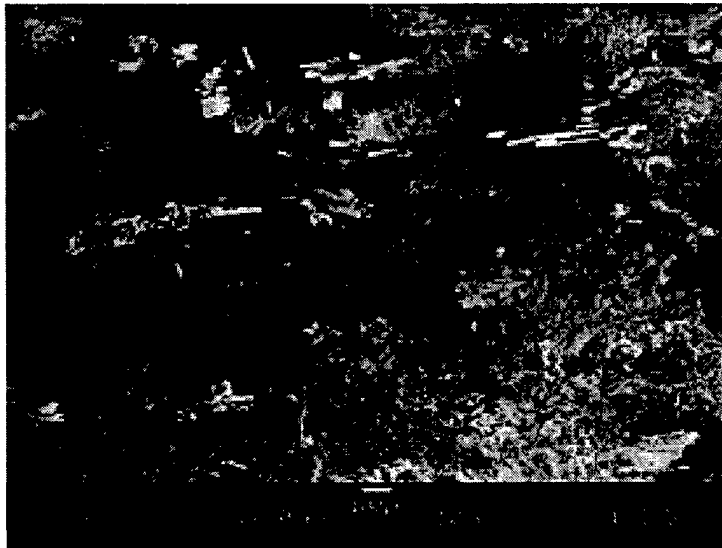**Figure 4.18** Room Temperature Monotonic Tensile Test SEM, 50X

The fractured surface of the elevated temperature monotonic tensile test specimen is shown in Figure 4.19. Scanning Electron Micrographs of the elevated temperature test specimen fracture surface are shown in Figures 4.20-4.22. The elevated temperature fracture surface edges, as can be seen in Figures 4.19 and 4.20, are slightly rough compared to the room temperature fracture surface edges and have some jagged growth pattern. Fiber pull-out is clearly noticeable, as can be seen in the protruding 90° yarns in Figure 4.21. Figure 4.22 is a high magnification SEM photomicrograph and displays a high degree of 90° yarn splitting and fiber pull-out. These are also evidence of matrix cracking, interface debonding, and fiber break.
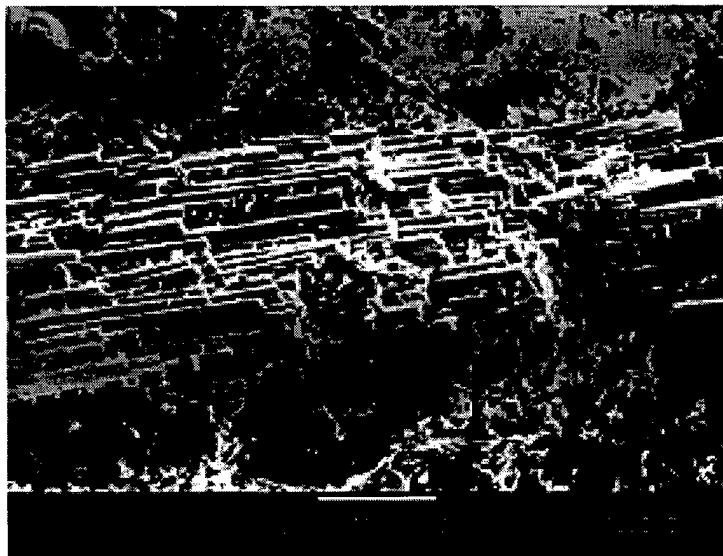

Figure 4.19 Elevated Temp. Monotonic Tensile Test Surface, Top View

Figure 4.20 Elevated Temperature Monotonic Test Fracture Surface SEM, 12X

Figure 4.21 Elevated Temperature Monotonic Test Fracture Surface SEM, 40X

Figure 4.22 Elevated Temp. Mono.Tensile Test Fracture Surface SEM, 200X

Overall comparison between the damage mechanisms in the test specimens under monotonic tensile loading at room and elevated temperatures shows that the elevated temperature promoted matrix cracking, interface debonding, and fiber break in the form of more yarn splitting and more fiber debonding in the 90° yarns . The fracture surface in the elevated temperature test has more roughness than the fracture surface in the room temperature test due to the presence of more fiber pull-out caused by the high temperature. The more jagged fractured surface means matrix cracking occured at infinitely many planes, then finally pulled the 90° yarn fibers more, or they were attached for longer time and hence higher strain. So, fiber pull-out caused by the elevated temperature allows the specimen to withstand higher values of strain to failure, and this is confirmed by the elevated temperature test failure strain, which was 0.247%; while the

room temperature test failure strain was 0.126%. In both tests the fracture extends perpendicular to the uniaxial load.
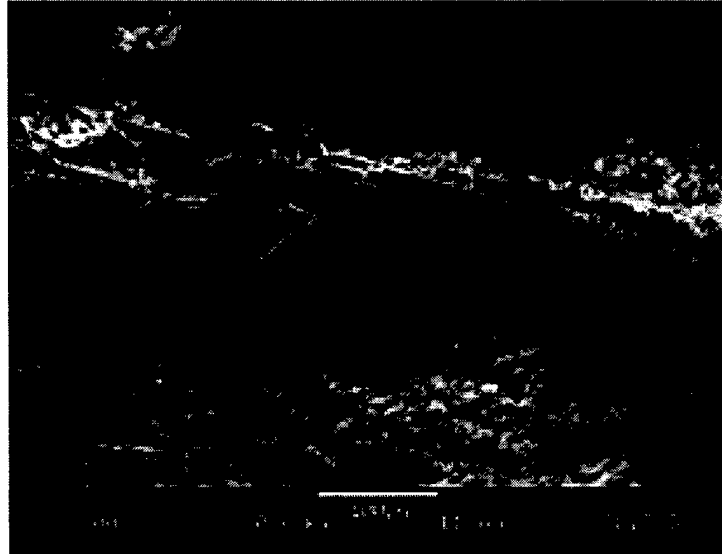
4.6.2. Monotonic Compression Tests

The fractured specimen and surface of the room temperature monotonic compression test is shown in Figure 4.23, and SEM micrographs are shown in Figures 4.24 & 4.25.
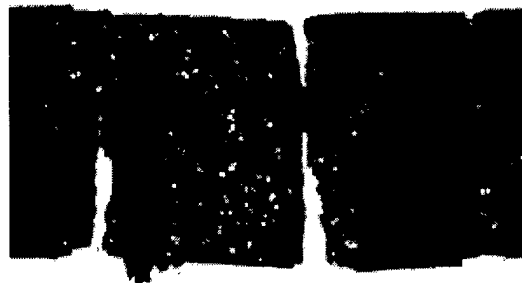

Figure 4.23 Room Temperature Monotonic Compression Specimen, Top View
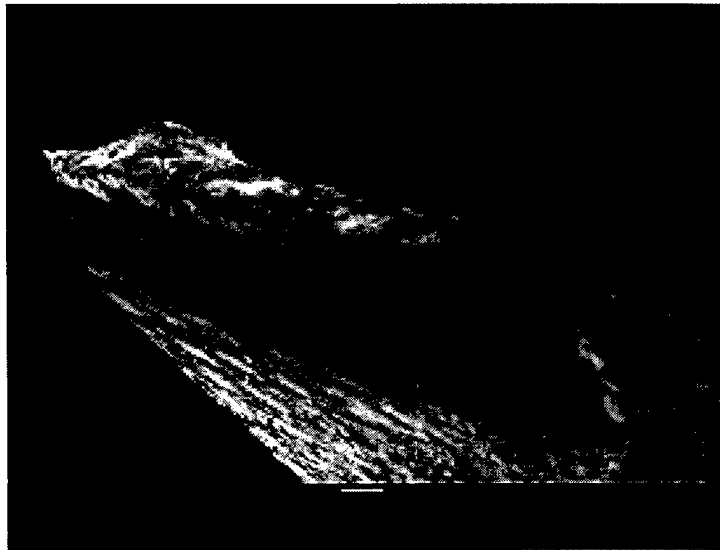
Figure 4.24 Room Temperature Comp. Test Fracture surface SEM, 15X Cross-Section Rotated 45° CW

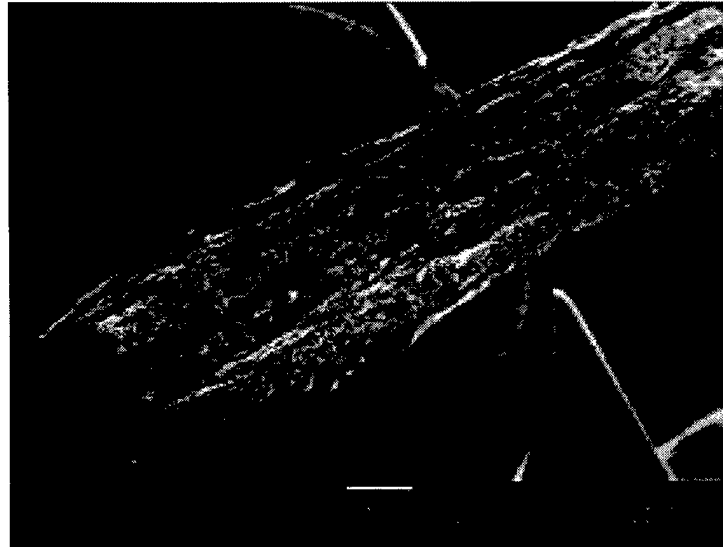**Figure 4.25** Room Temperature Comp.Test Fracture Surface SEM, 200X

Figure 4.26 Room Temperature Monotonic Comp. Test Fractured Pieces,
Top View

The fracture surface in this test as seen in figure 4.24 is very rough and is irregular. Both 0° & 90° yarns and matrix have broken. The matrix was crushed, and this was noticed as black powder coming out of the specimen at the fracture surface. Also, the specimen broke into pieces in the gage length, and these pieces came out of the upper and
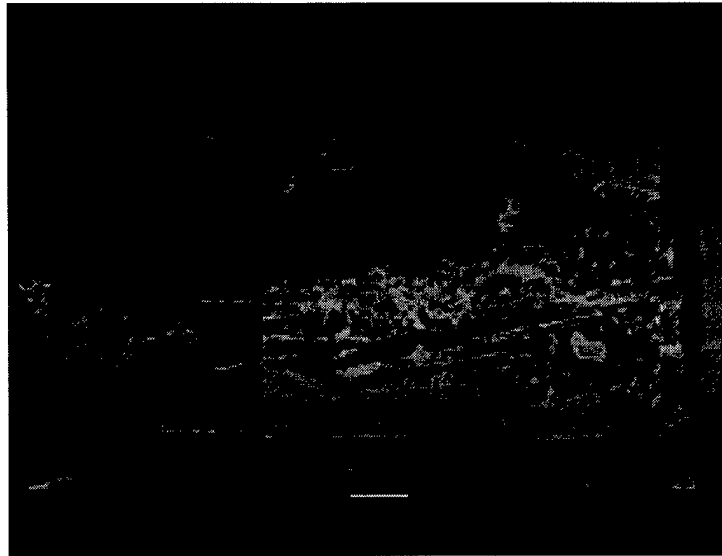
lower surfaces of the test specimen. Figure 4.25 shows both 0° and 90° yarns fractured and also matrix cracking within the yarn, interface debonding, and fiber breakage.
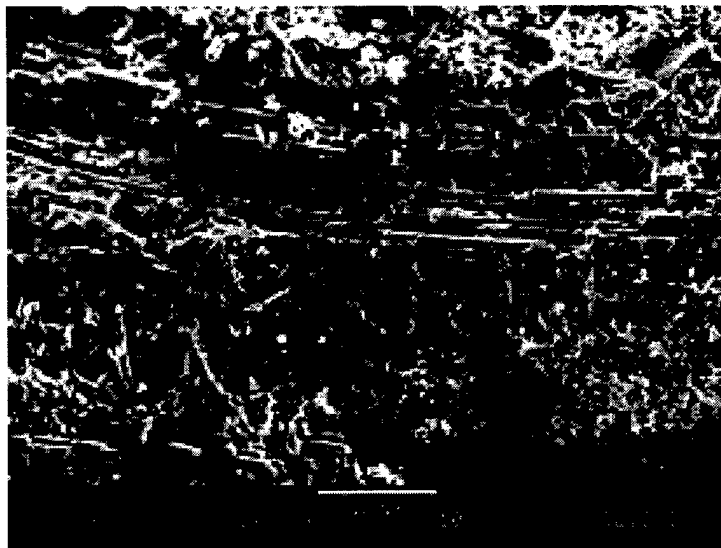

Figure 4.27 Elevated Temp. Comp. Test Fracture Surface, Top View

Figure 4.28 Elevated Temp. Comp. Test Fracture Surface, SEM, 11X
Cross-Section Rotated 45° CCW

Figure 4.29 Elevated Temperature Comp. Test Fracture Surface, SEM, 50X LH Side, 100X RH Side

Figure 4.30 Elevated Temp. Comp. Test Fracture Surface SEM, 200X

The elevated temperature specimen's fracture surface, as shown in Figure 4.27, is slightly smooth. 90°fiber pull-out and delamination are visible in this test with some matrix/fiber interface debonding, as can be seen in Figure 4.28. The elevated temperature effect on the specimen is noticed in Figures 4.29 and 4.30. The 90° yarn splitting on top of this figure is evident, along with matrix cracking, interface debonding, and fiber break.

On comparison, one can see that the damage to both fiber and matrix is less in the elevated temperature test than in the room temperature test. The fracture surface in the elevated temperature test has far less fiber break in the 90° yarn and matrix crushing than the room temperature test. Delamination is visible on the top and lower surfaces of the specimen in the elevated temperature test, while this area is crushed in the room temperature case. The amount of black powder that came out from the crushed matrix in the elevated temperature test was negligible compared to the amount that came out from the room temperature test. The pieces that broke off from the test specimen in the elevated temperature test are flake like pieces and are negligible compared to that in the room temperature test. The fracture surface as a whole in the elevated temperature test is less rough than that in the room temperature test, indicating that the elevated temperature has a positive effect on the monotonic compression characteristics. This effect is observed in the maximum stress to failure. The maximum stress to failure in the elevated temperature test is 334.5MPa, whereas it is 273.9MPa in the room temperature test with 60.6MPa difference. Also, the elevated temperature effect is noticeable in the maximum strain to failure in these tests, where it was 0.43% in the room temperature test and

0.5446% in the elevated temperature test with 0.1146% difference. This improved behavior of the material being investigated under elevated temperature compressive loading conditions make it suitable for future use in components that need to work under such conditions.

4.6.3. Room Temperature Tension-Tension Fatigue Tests

Three Tension-Tension fatigue tests were carried out at room temperature. Table 4.3 shows results of these tests.

Table 4.3. Room Temperature Tension-Tension Fatigue Tests

Maximum Stress Level (MPa)	Number of Cycles to Failure
40	40,000 (No Failure)
45	40,000 (No Failure)
50	10,922
52.5	11,310
55	1,618

Figures 4.31, 4.32 and 4.33 show photographs of the fractured specimens tested at 55, 52.5, and 50MPa maximum stress, respectively. The fracture surface of the 55MPa (80% of failure strength) maximum stress test is the roughest amongst the three tests. The 55MPa maximum stress fracture surface is similar to room temperature monotonic test fracture surface, with a lot of fiber pull-out in the 90° yarn fiber bundles, interface debonding, and matrix cracking, as seen in figure 4.34. The 52.5MPa test fracture surface is less rough, and the 50MPa test fracture surface is the smoothest of all these.

SEM micrograph of the 55MPa test specimen, as seen in Figure 4.35, shows that the fracture surface has a smooth region with very little fiber pull-out and a rough region with a lot of fiber pull-out. The smooth region, as shown in the left hand side of Figure

4.35, formed about 35% of the fracture surface cross section, and the rough region (in the right hand side), formed about 65% of the fracture surface cross section. The smooth region is due to fatigue failure in the form of multiple matrix micro-cracking, and the rough region is due to 90° yarn splitting, fiber pull-out, and matrix micro-cracking. The visible fibers in the 90° yarns are evidence of the 90° matrix micro-cracking and crack deflection along interface regions.

SEM micro-graphs of the 52.5MPa test fracture surface, Figures 4.37 and 4.38, show that the fracture surface has both a rough and a smooth region. The rough region in this test, which formed about 45% of the fracture surface, is less rough than the rough region in the 55MPa test; and the smooth region, which formed about 55% of the fracture surface, is smoother than that in the 55MPa test.

SEM micrographs of the 50MPa test fracture surface, Figures 4.39 and 4.40, also show that the fracture surface has a smooth and a rough region. The smooth region, as shown in Figure 4.39, has little fiber pull-out and formed about 75% of the fracture surface. The rough region, Figure 4.40, has a considerable amount of fiber pull-out and formed about 25% of the fracture surface. The first cycle in this test failed to activate all damage mechanisms, but the fatigue promoted the development of multiple matrix micro-cracking and fiber pull-out up to failure. Table 4.4 summarizes these results.

Table 4.4. Room Temperature Tension-Tension Fatigue Tests Fracture Surfaces Percentage

Test (Max. Stress/MPa)	Rough Area (%)	Smooth Area (%)
55	65	35
52.5	45	55
50	25	75

It can be concluded from these results that failure in the low cycle room temperature T-T fatigue test is due to matrix cracking, interface debonding, and fiber break of the 90° yarns. On the other hand, failure in the high cycle fatigue test is mainly due to fatigue in the form of multiple matrix micro-cracking, with some fiber pull-out of the 90° yarn.
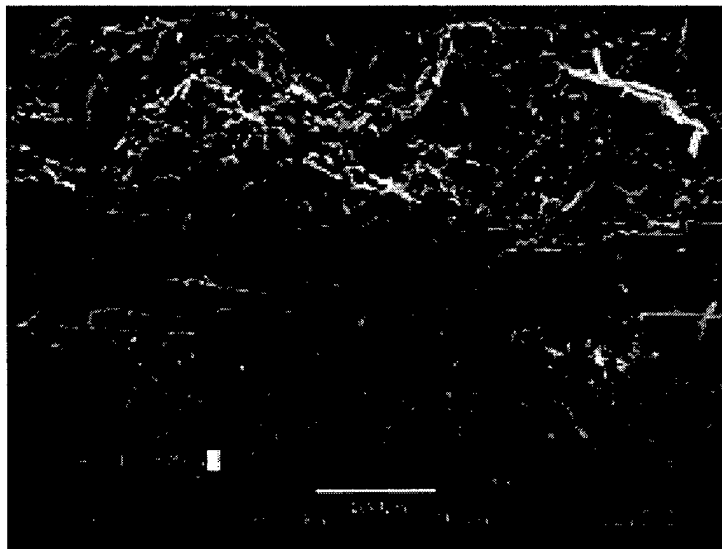

Figure 4.31 55MPa Max. Stress Room Temperature Tension-Tension Fatigue Test fracture Surface, Top View
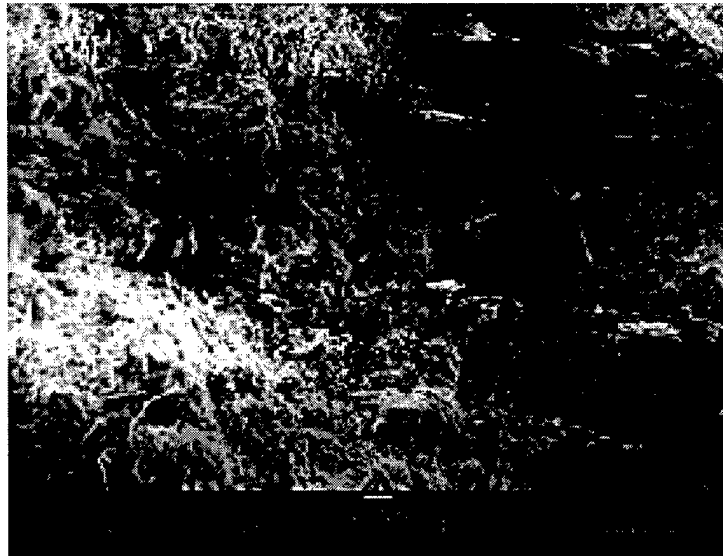

Figure 4.32 52.5MPa Max. Stress Room Temperature Tension-Tension Fatigue Test Fracture Surface Test, Top View
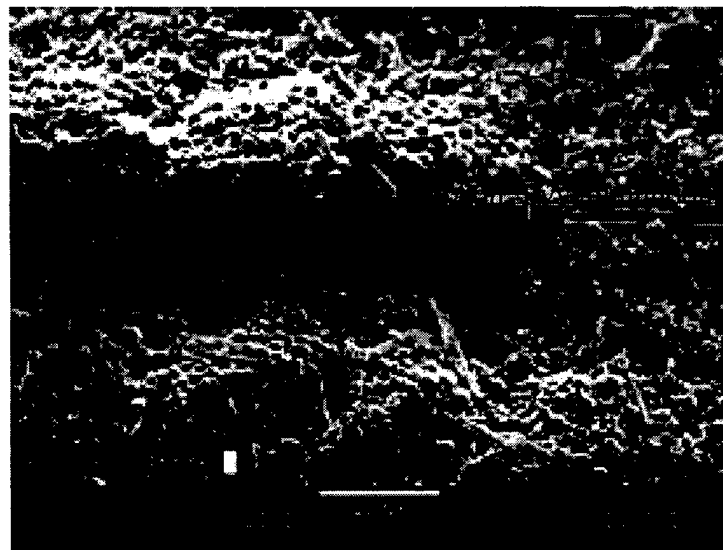
Figure 4.33 50MPa Max. Stress Room Temperature
Tension-Tension Fatigue Test Fracture Surface, Top View
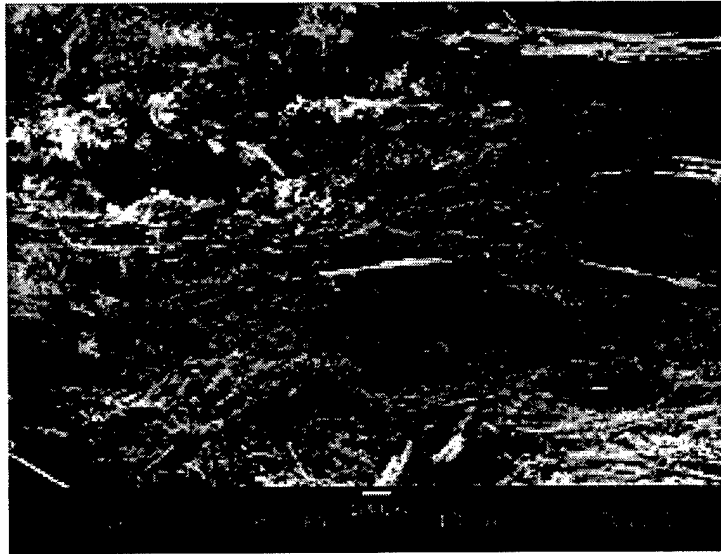

Figure 4.34 55MPa Room Temperature Tension-Tension
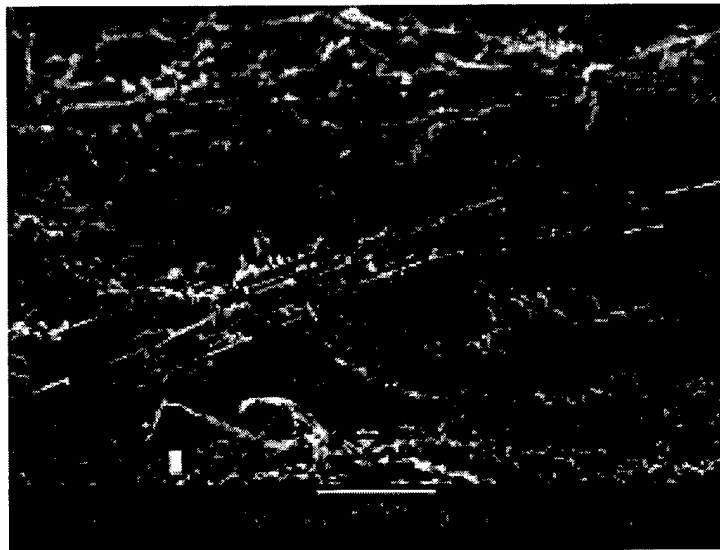Fatigue Test Rough Surface, SEM, 200X

Figure 4.35 55MPa Room Temperature Tension-Tension
Fatigue Test Fracture Surface, SEM, 50X
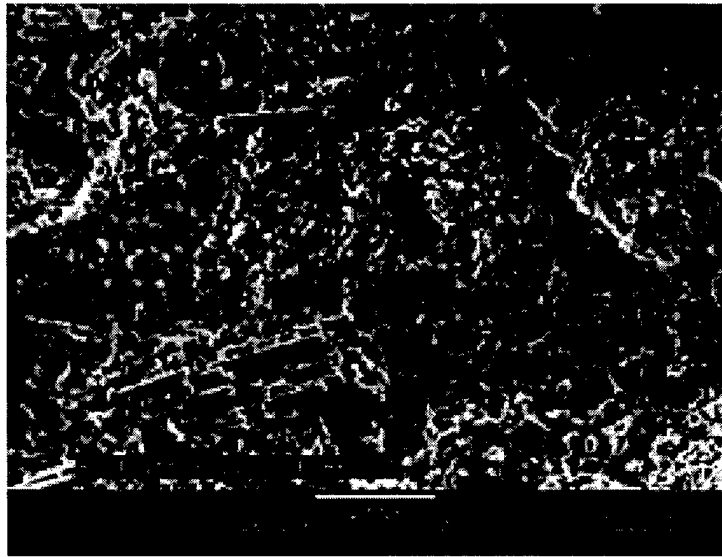

ùñ$ù÷2ùù!ññ†ñðõñý(ððaý

Figure 4.36 55MPa Room Temperature Tension-Tension
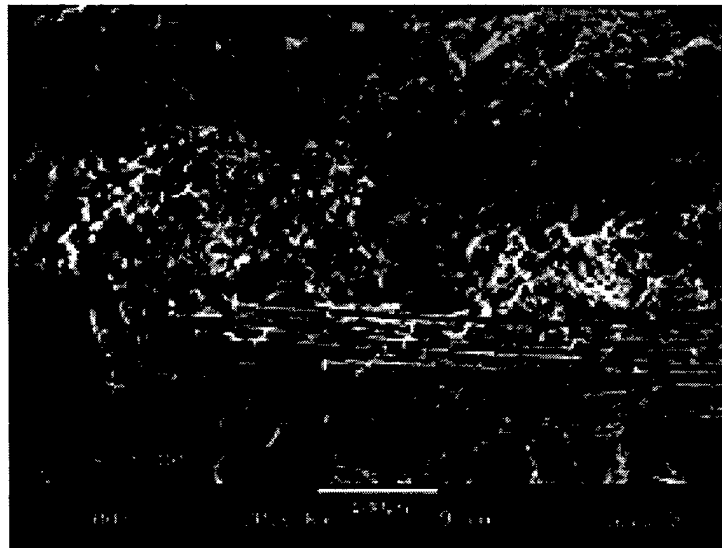Fatigue Test Smooth Surface, SEM, 200X

Figure 4.37 52.5MPa Room Temperature Tension-Tension
Fatigue Test, Rough Surface, SEM, 50X

Figure 4.38 52.5MPa Room Temperature Tension-Tension
Fatigue Test Smooth Surface, SEM, 200X

53

Figure 4.39 50MPa Room Temperature Tension-Tension
Fatigue Test Smooth Surface, SEM, 200X

Figure 4.40 50MPa Room Temperature Tension-Tension
Fatigue Test Rough Surface, SEM, 200X

4.6.4. Elevated Temperature Tension-Tension Fatigue Tests

Elevated temperature tension-tension fatigue tests were carried out at 760°C. Four tests of this kind were conducted at 40, 30, 25, and 20MPa maximum stress levels. Table 4.5 below shows these tests and the corresponding number of cycles to failure.
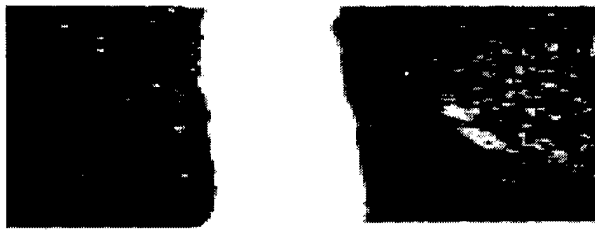
Table 4.5. Elevated Temperature Tension-Tension Fatigue Tests

Maximum Stress (MPa)	Cycles to Failure
40	2,210
30	15,710
25	15,540
20	30,427

The fracture surfaces of the test specimens used for these tests are shown in Figures 4.41, 4.42, 4.43, and 4.44. It is clearly seen from these figures that the high stress low cycle fatigue test fracture surface (40MPa max. stress) is the roughest one, has slightly jagged edges, and is similar to the elevated temperature monotonic tensile test fracture surface discussed earlier. The fracture surface roughness and the jagged pattern of its edges decrease as the maximum fatigue stress is decreased. Figures 4.45 and 4.46 show that the 90° yarns have fractured. This involves matrix cracking within the yarns, fiber breakage and pull-out, yarn splitting, and interface debonding. The level of fiber pull-out, interface debonding and matrix cracking decreases with the test maximum stress level, as can be seen from Figures 4.45-4.52 Figure 4.49 is a 200X SEM micrograph of the 20MPa maximum stress test specimen and shows that there is less yarn splitting and hence less 90° fiber pull-out and less matrix cracking at this low maximum stress level. The failure in this test is due mainly to fatigue in the form of multiple matrix micro-

cracking with the fractured surface being very smooth, as seen in Figure 4.52. It is worth noting that, in these tests, there are no smooth and rough regions in the fracture surface as was seen previously in the room temperature T-T fatigue tests. The white mark on some of these pictures is the white adhesive used to hold the thermocouples in place on the test specimen during testing. The maximum and minimum strain curves for these tests, Figure 4.12, indicate that creep has occured in the test specimen. This is in agreement with what was said about the 90° yarns failure in the form of fiber pull-out and interface debonding. Fiber pull-out and interface debonding increased with fatigue cycling until failure.

On comparison, it can be seen that the elevated temperature T-T fatigue tests have more 90° yarn failure as fiber pull-out, matrix cracking, and interface debonding than the room temperature T-T fatigue tests. The residual strain has increased in all of these tests indicating some micro-structural damage accumulation or creep. This is an indication that the material under investigation can withstand higher values of strain at elevated temperatures preventing catastrophic failure under similar loading conditions. Significant damage occured on the first cycle of the room and elevated temperatures fatigue tests. After this first cycle damage, there is strain accumulation in the elevated temperature fatigue tests indicating permanent deformation as a result of the cyclic loading. In the room temperature fatigue tests, the strain remained almost constant as cycling progressed up to failure. The lack of fiber pull-out in the low stress high cycle fatigue tests at both test temperatures reverted to the undesirable CMCs failure mode.

Figure 4.41 40MPa Elevated Temperature Tension-Tension
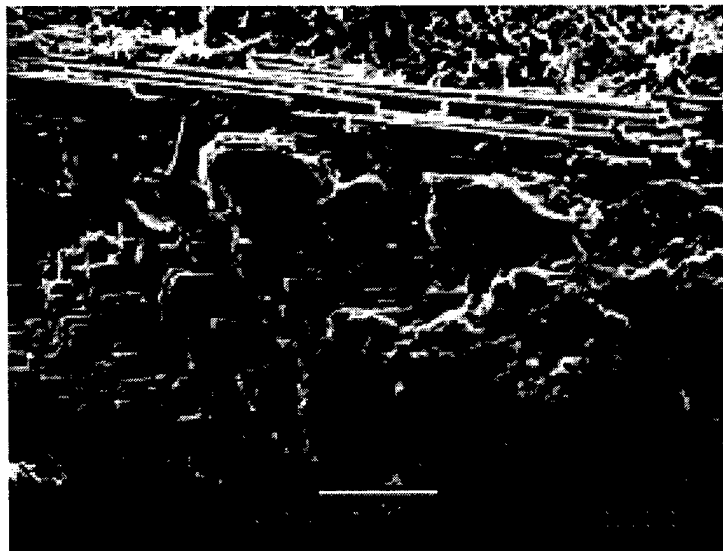Fatigue Test Fracture Surface, Top View

Figure 4.42 30MPa Elevated Temperature Tension-Tension
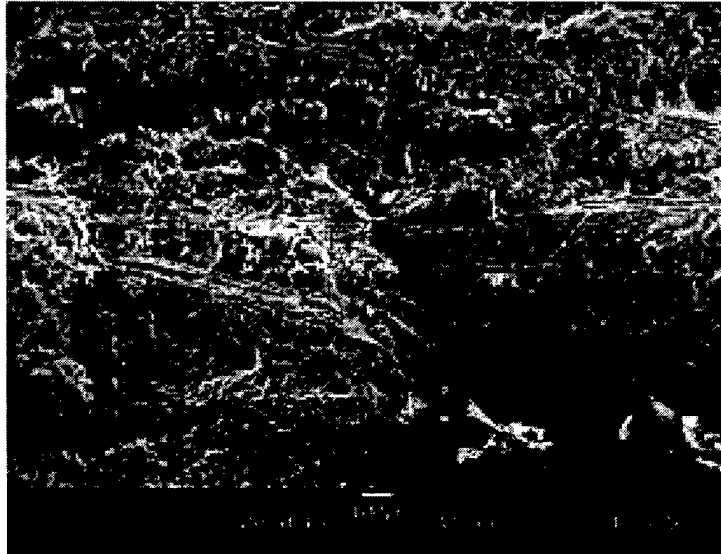Fatigue Test Fracture Surface, Top View

Figure 4.43 25MPa Elevated Temperature Tension-Tension
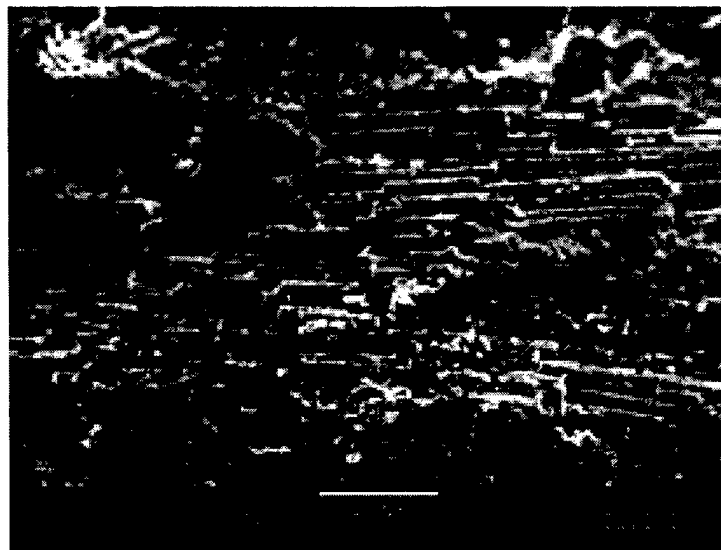Fatigue Test Fracture Surface, Top View

Figure 4.44 20MPa Elevated Temperature Tension-Tension
Fatigue Test Fracture Surface, Top View

Figure 4.45 40MPa Elevated Temperature Tension-Tension
Fatigue Test Fracture Surface SEM, 200X

Figure 4.46 40MPa Elevated Temperature Tension-Tension
Fatigue Test Fracture Surface SEM, 50X

Figure 4.47 30MPa Elevated Temperature Tension-Tension
Fatigue Test Fracture Surface SEM, 200X

Figure 4.48 20MPa Elevated Temperature Tension-Tension
Fatigue Test Fracture Surface SEM, 50X
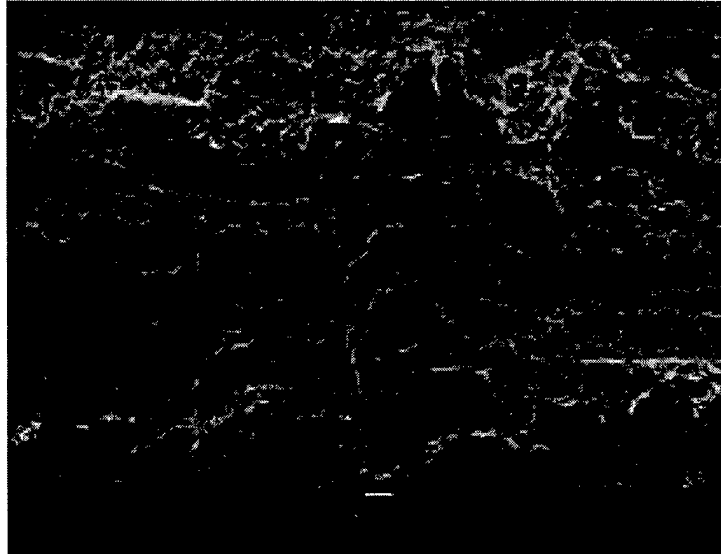

Figure 4.49 20MPa Elevated Temperature Tension-Tension
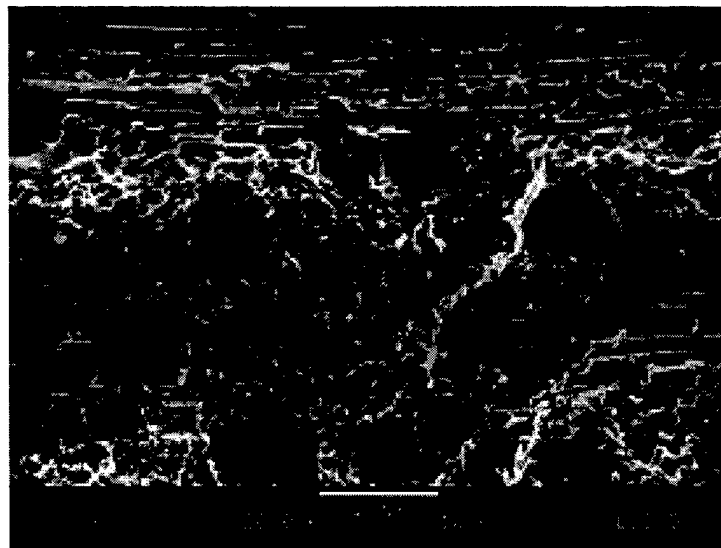Fatigue Test Fracture Surface SEM, 200X

Figure 4-50 40MPa Elevated Temperature Tension-Tension
Fatigue Test Fracture Surface SEM, 15X

Figure 4-51 30MPa Elevated Temperature Tension-Tension
Fatigue Test Fracture Surface SEM, 15X

Figure 4-52 20MPa Elevated Temperature Tension-Tension
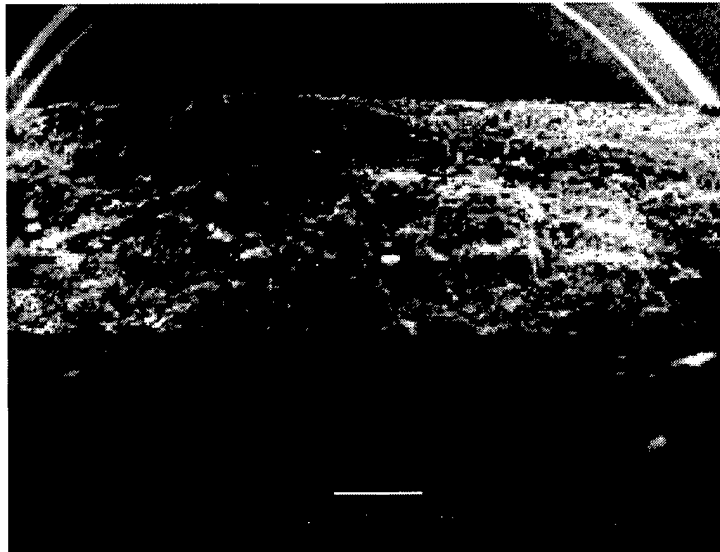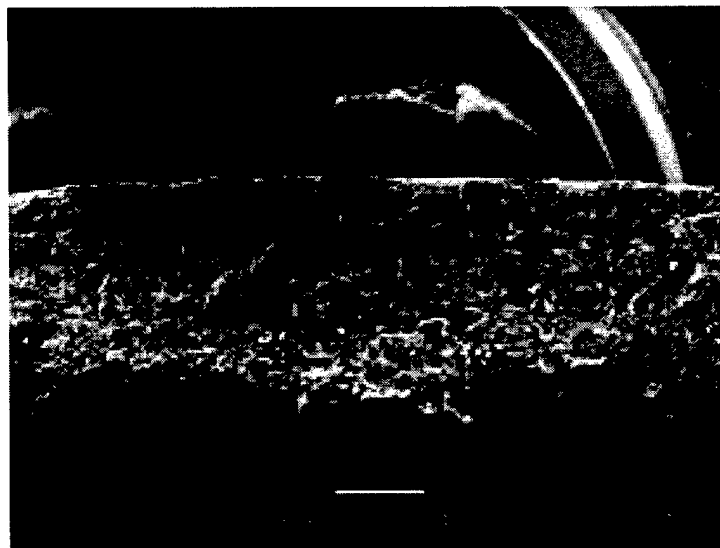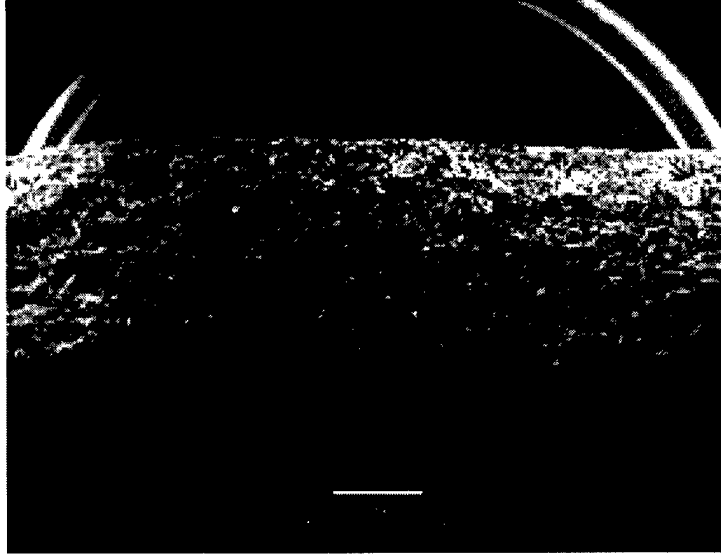Fatigue Test Fracture Surface SEM, 15X

4.6.5. Room Temperature Tension-Compression Fatigue Tests

These tests were carried out at a maximum to minimum load ratio of -1. Table 4.6

summarizes these tests.

Table 4.6. Room Temperature Tension-Compression Fatigue Tests

Max. Stress (MPa)	Cycles To Failure
45	162
40	11096
35	40,000 (No Failure)

The fracture surfaces of the 45 & 40MPa are shown in Figures 4.53 and 4.54. The

45MPa test fracture surface is relatively rough and is slightly jagged, while the 40MPa

test fracture surface is smoother with little fiber pull-out . This difference in the fracture

surface characteristics is also visible in the 15X SEM micrographs shown in Figures 4.55

and 4.56, with the 45MPa test fracture surface having more fiber pull-out and matrix cracking than the 40MPa test fracture surface.

The 50X fracture surface SEM micrograh of the 45MPa test, Figure 4.57, shows severe fiber pull-out in the 90° yarn, matrix cracking, and interface debonding. These are the causes of failure in the low cycle fatigue test. Less fiber pull-out in the 90° yarn is clearly noticeable in the 50X fracture surface SEM micrograh of the 40MPa test. Failure of the test specimen in this high cycle fatigue test is mainly due to fatigue in the form of multiple matrix micro-cracking, and some fiber pull-out in the 90° yarn, matrix cracking, and interface debonding. The failure mechanism in the low cycle room temperature T-C fatigue test is in close agreement with the failure mechanism in the room temperature monotonic compression test.
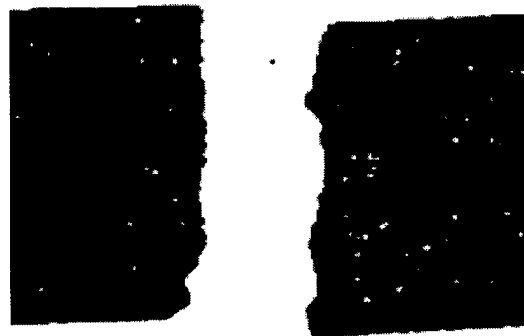
Figure 4.53 45MPa Room Temperature Tension-Compression
Fatigue Test Fracture Surface, Top View

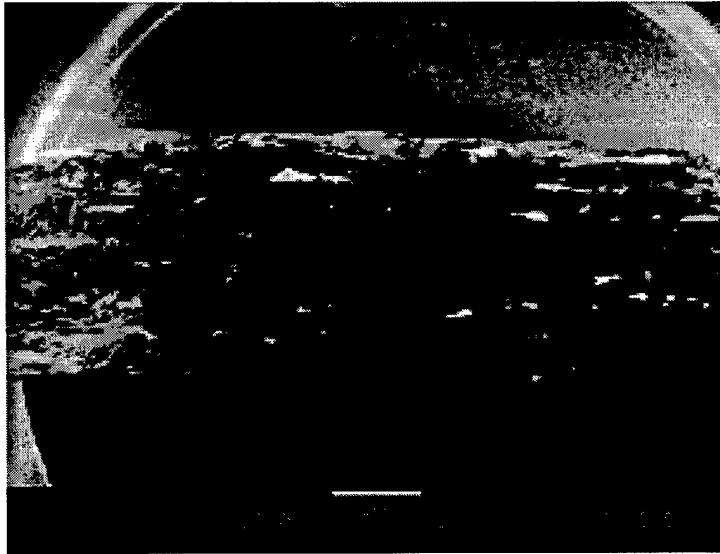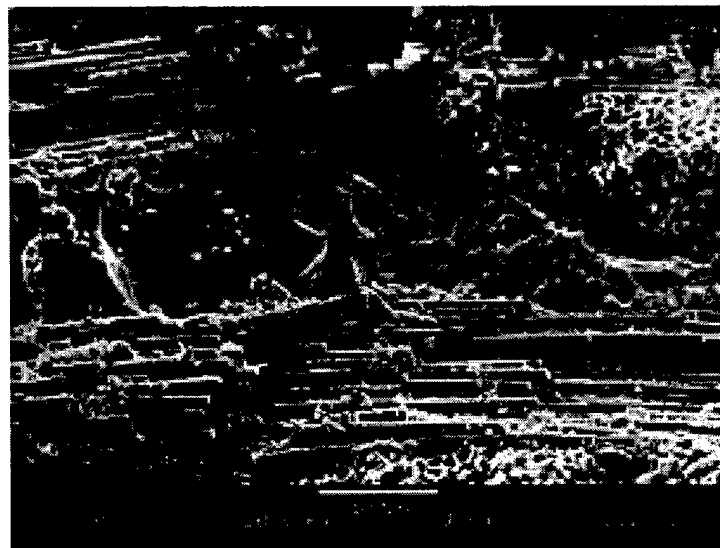**Figure 4.54** 40MPa Room Temperature Tension-Compression
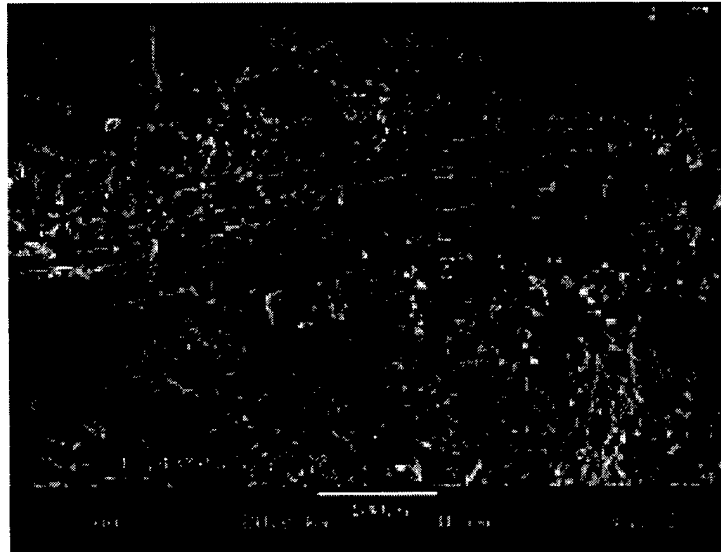Fatigue Test Fracture Surface, Top View

Figure 4.55 45MPa Room Temperature Tension-Compression
Fatigue Test Fracture Surface SEM, 15X

Figure 4.56 40MPa Room Temperature Tension-Compression
Fatigue Test Fracture Surface SEM, 15X

Figure 4.57 45MPa Room Temperature Tension-Compression
Fatigue Test Fracture Surface SEM, 200X

65

Figure 4.58 40MPa Temperature Tension-Compression
Fatigue Test Fracture Surface SEM, 200X

4.6.6. Elevated Temperature Tension-Compression Fatigue Tests

These tests were conducted at 760°C at a maximum to minimum load ratio of -1.

Table 4.7 summarizes these tests.

Table 4.7. Elevated Temperature Tension-Compression Fatigue Tests

Maximum Stress Level (MPa)	Cycles to Failure
40	1407
30	10315
25	16086
20	40,000 (No Failure)

The fracture surfaces of the 40, 30, and 25MPa tests are shown in Figures 4.59,

4.60, and 4.61. The 40MPa test fracture surface is the roughest, followed by the 30 and

then the 25MPa test, which is the smoothest. The low cycle high stress fatigue test SEM

micro-graph, Figure 4.62, shows some 90° yarn splitting, indicting that matrix cracking, interface debonding, and fiber pull-out are the main damage mechanisms. This is similar to the failure mechanism due to monotonic compression at the elevated temperature. Less damage of this kind is present in the intermediate cycle fatigue test, Figure 4.66. The high cycle fatigue test SEM micro-graph shows no signs of fiber pull-out in the 90° yarn or matrix cracking. The damage in this low stress high cycle fatigue test is due to fatigue in the form of multiple matrix micro-cracking that caused eventual failure.

Comparison between room and elevated temperature T-C fatigue tests reveals that there is more fiber pull-out in the 90° yarn, matrix cracking, and interface debonding at room temperature than at the elevated temperature. Failure in these fatigue tests at room and elevated temperatures was in tension for all the test specimens that failed.
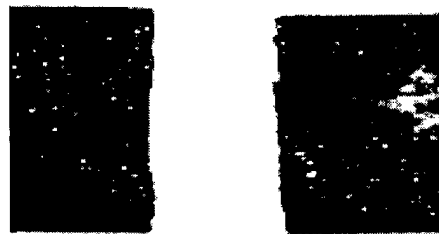
Figure 4.59 40MPa Elevated Temperature Tension-Compression
Fatigue Test Fracture surface, Top View
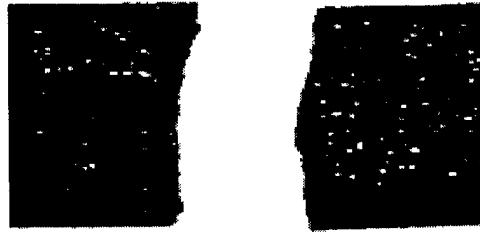
Figure 4.60 30MPa Elevated Temperature Tension-Compression
Fatigue Test Fracture surface, Top View
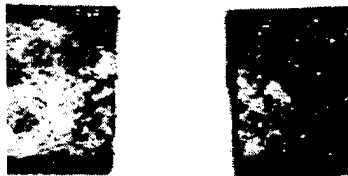
Figure 4.61 25MP Elevated Temperature Tension-Compression
Fatigue Test Fracture surface, Top View

Figure 4.62 40MPa Elevated Temperature Tension-Compression
Fatigue Test Fracture Surface SEM, 15X

Figure 4.63 30MPa Elevated Temperature Tension-Compression
Fatigue Test Fracture Surface SEM, 20X

Figure 4.64 25MPa Elevated Temperature Tension-Compression
Fatigue Test Fracture Surface SEM, 15X

Figure 4.65 40MPa Elevated Temperature Tension-Compression
Fatigue Test Fracture Surface SEM, 200X
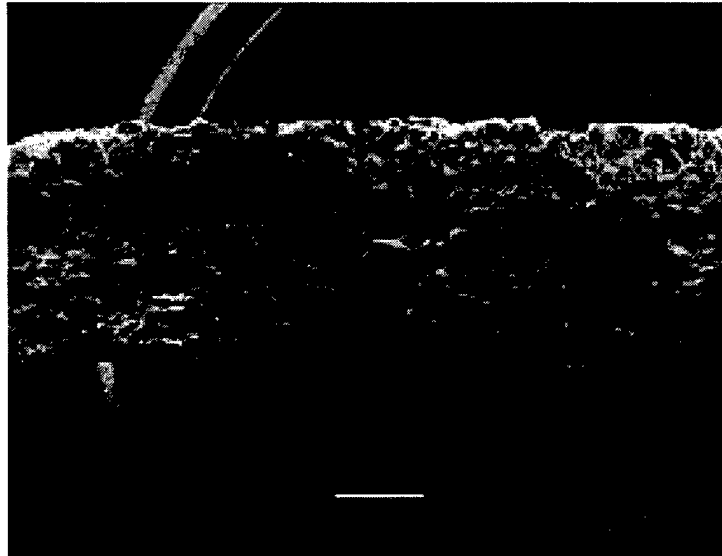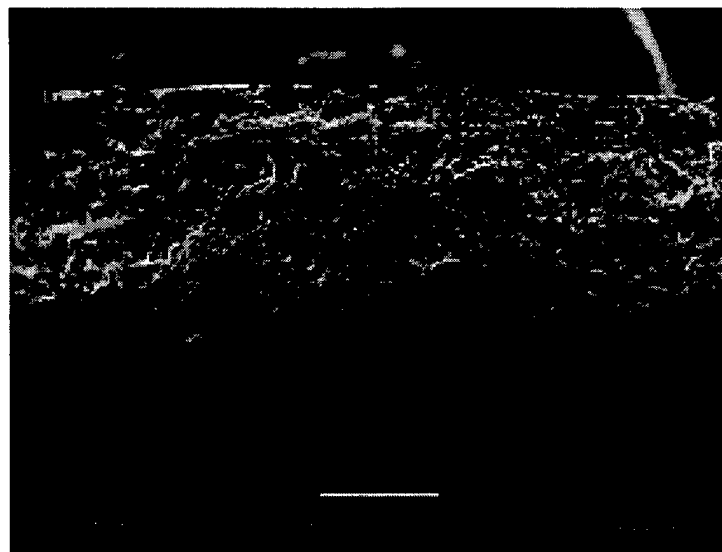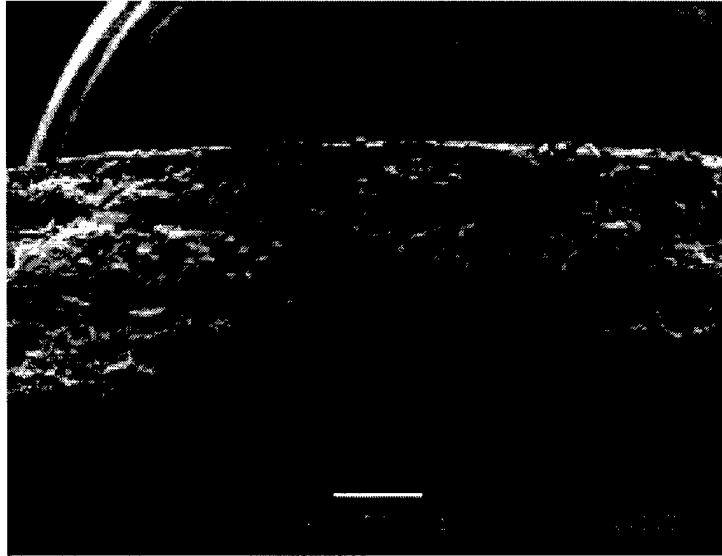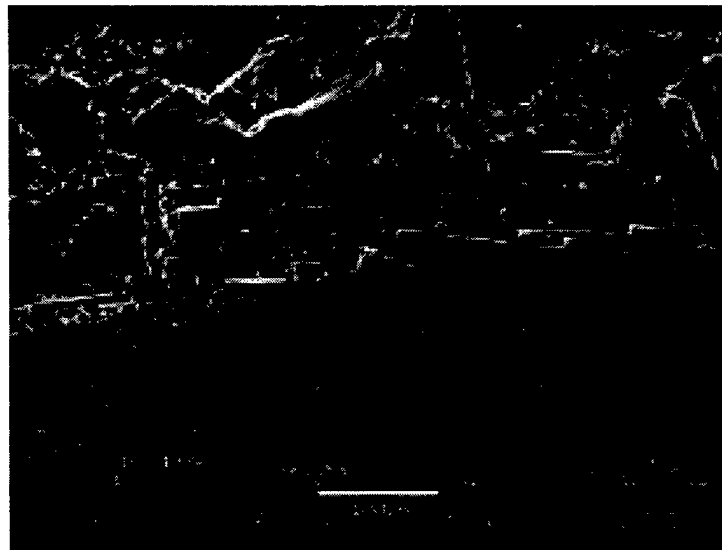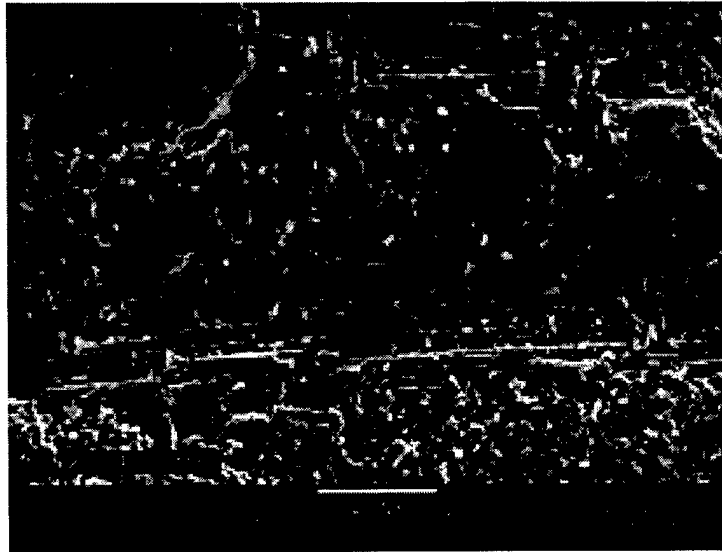
Figure 4.66 30MPa Elevated Temperature Tension-Compression
Fatigue Test Fracture Surface SEM, 200X

Figure 4.67 25MPa Elevated Temperature Tension-Compression
Fatigue Test Fracture Surface SEM, 200X

5. CONCLUSIONS

In summary, the main purpose of this study was to investigate the monotonic and fatigue behavior of a 2-D Blackglas/Nextel nitrided 312 woven fabric ceramic matrix composite (CMC) at room and elevated temperatures. The elevated temperature was 760°C. The behavior of the Blackglas/Nextel composite was determined for monotonic tension and compression, tension-tension, and tension-compression fatigue loading at room and elevated temperatures. Tension-tension fatigue tests were conducted at a minimum to maximum load ratio of 0.05 and the tension-compression fatigue tests were conducted at a minimum to maximum load ratio of -1. S-N curves were obtained to determine the fatigue life of the material under tension-tension and tension-compression loading at room and elevated temperatures. The failure mechanisms were investigated for all of the tests conducted. Both monotonic, and fatigue tests were conducted in a load controlled mode and employed a triangular load wave and a frequency of 0.1Hz.

The stress-strain curve for the room temperature monotonic tensile test showed a linear response up to 44MPa stress level. The ultimate strength was 69.4MPa, and the ultimate strain was 0.1261%. The Young's modulus of elasticity calculated from the linear region was 62.8GPa. At the elevated temperature, the stress-strain curve showed a proportional limit of 24MPa. The ultimate strength was 65.2MPa, and the ultimate strain was 0.2474%. The Young's modulus of elasticity calculated from the linear region was 57.6GPa. The fractured surface of the elevated temperature monotonic tensile test specimen had more fiber pull-out in the 90° yarn, more matrix cracking, and more

interface debonding than the room temperature monotonic tensile test specimen fractured surface.

Under monotonic compression loading, the material exhibited a linear behavior up to failure at both test temperatures. The room temperature ultimate strength was 273.9MPa and the failure strain was 0.43%. The Young's modulus of elasticity calculated from the room temperature test was 62.5GPa. This value of Young's modulus is the same as the value obtained from the room temperature monotonic tension test (62.8GPa). The elevated temperature ultimate strength was 334.5MPa and the failure strain was 0.5446%. The Young's modulus of elasticity calculated from the elevated temperature monotonic compression test was 60.5GPa. This value of Young's modulus is again, comparable to the value obtained from the elevated temperature monotonic tension test. The test specimen had less fiber break in the 90° yarn and matrix damage, and greater failure strain at the elevated temperature than at the room temperature. Overall, the material showed better behavior under compressive loading at the elevated temperature than at room temperature.

S-N curves of the tension-tension fatigue tests showed that the material has a fatigue strength for 40,000 cycles of 48MPa at room temperature and 24MPa at the elevated temperature. Both room and elevated temperatures high stress/low cycle fatigue tests fractured surfaces experienced high levels of fiber pull-out in the 90 ° yarns, matrix cracking, and interface debonding. These failure modes were more noticeable at the elevated temperature. On the other hand, the low stress/high cycle fatigue tests fractured surfaces were smooth and showed little or no signs of fiber pull-out, matrix cracking, or

interface debonding. Failure in these tests was due to progressive fatigue damage . Strain curves of the room temperature tension-tension fatigue tests showed an initial value of strain due to the first cycle, and this value of strain remained constant with cycling up to failure. Strain curves of the elevated temperature tension-tension fatigue tests showed that both minimum and maximum strains increased at the same rate, indicating that creep was occurring in the material as cycling progressed.

S-N curves of the tension-compression fatigue tests showed that the material had a fatigue strength for 40,000 cycles of 36MPa at room temperature and 24MPa at the elevated temperature. The high stress/low cycle tests fractured surfaces were rough at both room and elevated temperatures with fiber break, matrix cracking, and interface debonding. The room temperature tests showed more of these failure mechanisms than the elevated temperature tests. On the other hand, the low stress/high cycle fatigue tests fractured surfaces were smooth and showed little or no signs of fiber pull-out, matrix cracking, or interface debonding. Failure in these tests was due to fatigue. All tension-compression test specimens that did not survive cycle run-out limit of 40,000 cycles failed in tension mode. Both, room and elevated temperature minimum and maximum strain curves showed an initial strain value upon the onset of cycling, and this value remained fairly constant as cycling progressed up to failure.

S-N curves showed that the material had higher fatigue life in tension-tension than in tension-compression at a given maximum stress level at room temperature conditions. Also, these curves showed that the material had the same fatigue life at the elevated temperature under tension-tension and under tension-compression fatigue loading.

6. RECOMMENDATIONS

The room temperature and the 760°C monotonic tension and compression, tension-tension and tension-compression fatigue behavior of Nextil 312/Blackglas is now well known. The next step will be to determine the compression-compression and thermomechnical fatigue behavior of this low cost ceramic matrix material. The effects of temperature cycling could produce potentially unique behavior. Another potential study would be to determine the material tension-compression fatigue behavior using higher and lower R values.

Bibliography

1. André Rodrigues, L. Guerra Rosa, and M. Steen. "Fatigue Behavior of A Ceramic Matrix Composite, 2D C$_{fiber}$ / SIC$_{matrix}$," *The American Ceramic Society*, Vol. 57 , 1995, p 351-356 .

2. Stephen F. Shuler, John Wholmes, and Xin Wu. "Influence of loading Frequency on the Room-Temperature Fatigue of a Carbon-Fiber/SiC-Matrix Composite," *Journal of American Ceramic Society* Vol. 76 N.9, p 2327-2336 , 1993 .

3. Gerald Camus, Laurent Guillaumat, and Stephane Baste. "Development of Damage in a 2D woven C/SiC Composite under Mechanical Loading: I. Mechanical Characterization," *Composites Science and Technology*, Vol. 56, 1996, p 1363-1372 .

4. S. S. Campbel and S. T. Gonczy. "In-Situ Formation of Boron Nitride Interfaces on Nextel 312^{TM}/ BlackGlas^{TM} Continuous Ceramic Fiber I: Nitriding Process and BlackGlas^{TM} Ceramic Matrix Composite Properties," *Journal of Ceramic Engineering and Science Proceedings*, 15 [4], 327-336, (1994) .

5. S. S. Campbel and S. T. Gonczy. "In-Situ Formation of Boron Nitride Interfaces on Nextel 312^{TM}/ BlackGlas^{TM} Continuous Ceramic Fiber I: Oxidation of BlackGlas^{TM} Ceramic Matrix Composite," *Journal of Ceramic Engineering and Science Proceedings*, 15 [4], 337-343, (1994) .

6. K. Ranji Vaiduanathan, W. Roger Cannon, Stephen Danforth, Albert G. Tobin, and John Holmes. "Effect on Oxidation on The Mechanical Properties of Nextel 312^{TM}/BN/ BlackGlas^{TM}," *Materials Research Society Symposium Proceedings*, Vol. 365 (1995), p 429-434 .

7. K. Ranji Vaidyanathan, Jagannathan Sankar, and Ajit D. Kelkar. "Mechanical properties of Nextel 312^{TM} fiber-reinforced SIC Matrix Composites in tension," *Journal of Ceramic Engineering and Science Proceedings*, 15 [4], 251-261, (1994) .

8. K. Ranji Vaidyanathan, W. Roger Cannon, Stephen Danforth. "Creep resistance of Nextel 312^{TM}/BN/ BlackGlas^{TM}" Composites," *Journal of Ceramic Engineering and Science Proceedings*, vol. 16, p 549-557, 1995 .

9. S. S. Campbel, S. t. Gonczy, M. McNallan, and A. Cox. "Performance of Blackglas Composites in 4000-hour Oxidation Study," *Journal of Ceramic Engineering and Science Proceedings*, Vol. 17 [4-5], (1995), p 411-420 .

10. A. Tobin, J. Holmes, K. R. Vaidyanathan, W.R.Cannon, and S.C. Danforth. "Effects of Processing, Oxidation, & Fiber Architecture on Thermal & Mechanical Properties of BN-Nextel 312^{TM}/ Blackglas^{TM} Composites," *Journal of Ceramic Engineering and Science Proceedings*, Vol. 16, p 233-2242, 1995 .

11. M. N. Ghasemi Nijhad, and Jocelyn K. Bayliss. "Processing and Performance of Continuous fiber Ceramic Composites Using Vacuum Assisted Resin Transfer Molding And BlackGlas^{TM} Preceramic Polymer Pyrolysis," *Journal of Ceramic Engineering and Science Proceedings*, Vol.18 [3], p 391-399, 1997 .

12. S. Campbell, Edgar Leone, and Mike McNallan. "The effect of Processing Parameters On The Surface Nitridation Of Nextel 312^{TM} Ceramic," *Journal of Ceramic Engineering and Science Proceedings*, vol.18 [4], p 391-395, 1997

13. Daniel. J. Groner. "Characterization of fatigue Behavior of a 2-D Woven Fabric Reinforced Ceramic Matrix Composite at Elevated Temperature," *MS Thesis, AFIT/GAE/ENY/94D-15*, Air Force Institute of Technology (AU), Wright Patterson Air Force Base, OH, December 1994.

14. Frank A. Opalski. "Fatigue behavior of a cross-ply Ceramic Matrix Composite Under Tension-Tension & Tension-Compression Loading," *MS Thesis, AFIT/GAE/ENY/92-02,* Air Force Institute of Technology (AU), Wright Patterson Air Force Base, OH, February 1992 .

VITA

Musa Al-Hussein is a Lieutenant Colonel in the Royal Jordanian Air Force. He was born on April 18-1960 in Rasun, Ajlun. He graduated from Ajlun Secondary School in Ajlun, Jordan, in 1978. After secondary school he attended the University of Southampton, England where he earned a Bachelor of Science degree in Aeronautical Engineering in 1983. He then was commissioned in the Royal Jordanian Air Force in July 1983.

Lieutenant Colonel Al-Hussein was an Aeronautical Engineer in the Aircraft Maintenance Branch at King Hussein Air College. He was a Distinguished Graduate of the Aircraft Maintenance Officer Course in 1985, Shanute Air Force Base, IL. In 1987 he was selected as a technical representative for the Jordanian Air Force at the CASA-101 Aircraft Assembly Plant, Madrid, Spain. He was then appointed OIC, aircraft maintenance branch, King Hussein Air College, where he was in charge of maintaining the C-101, F-5, Bulldog, and Hughes aircraft. He was a member of the pilot selection committee 1990,1991, and 1992. In 1992 he was transferred to the Air Lift Wing where he served as chief of maintenance branch until September 1996. In September 1996 he entered the School of Engineering, Air Force Institute of Technology. During his career in the Jordanian Air Force, he participated in product improvement studies and projects. Lieutenant Colonel Al-Hussein holds the Technical Achievement and Deserve Medals.

Rasun,
Ajlun,
Jordan, 26823

REPORT DOCUMENTATION PAGE

Form Approved
OMB No. 0704-0188

1. AGENCY USE ONLY *(Leave blank)*	2. REPORT DATE	3. REPORT TYPE AND DATES COVERED
	September 1998	Master's Thesis

4. TITLE AND SUBTITLE
Monotonic and Fatigue Behavior of 2-D Woven Ceramic Matrix Composite at Room and Elevated Temperatures (Blackglas/Nextel 312)

5. FUNDING NUMBERS

6. AUTHOR(S)
Musa Al-Hussein, Lt Col, Royal Jordanian Air Force

7. PERFORMING ORGANIZATION NAME(S) AND ADDRESS(ES)
Air Force Institute of Technology
2950 P Street
WPAFB OH 45433-7765

8. PERFORMING ORGANIZATION REPORT NUMBER

AFIT/GAE/ENY/98-01

9. SPONSORING/MONITORING AGENCY NAME(S) AND ADDRESS(ES)
Dr. Ozden Ochoa   (202)767-0470
AFOSR/NA
110 Duncan Ave, Ste B115
Bolling AFB DC 20332-0001

10. SPONSORING/MONITORING AGENCY REPORT NUMBER

11. SUPPLEMENTARY NOTES
Dr. Shankar Mall, AFIT/ENY, 937-255-3636 Ext 4587

12a. DISTRIBUTION AVAILABILITY STATEMENT
Unclassified; distribution unlimited.

12b. DISTRIBUTION CODE

A

13. ABSTRACT *(Maximum 200 words)*

This study investigated the monotonic tension and compression and the tension-tension and tension-compression fatigue loading of Blackglas/Nextel 312 woven CMC at room temperature and at 760 degrees centigrade. Young's Modulus and strain variation were evaluated. S-N curves were obtained for room and elevated temperatures. The ultimate tensile stress was lower at the elevated temperature and it was higher in the compression test. Failure-strain was higher at the elevated temperature in both tension and compression tests. There was no significant change in Young's Modulus at the elevated temperature. Also, there was no difference in the number of cycles to failure at the elevated temperature between tension-tension and tension-compression fatigue loading. Microscopic examination was performed to characterize damage mechanisms. During monotonic and low cycle/high stress, far more fiber/interface debond was evident then in the high cycle/low stress fatigue tests.

14. SUBJECT TERMS

15. NUMBER OF PAGES
92

16. PRICE CODE

17. SECURITY CLASSIFICATION OF REPORT	18. SECURITY CLASSIFICATION OF THIS PAGE	19. SECURITY CLASSIFICATION OF ABSTRACT	20. LIMITATION OF ABSTRACT
Unclassified	Unclassified	Unclassified	UL